Core complex exhumation in peri-Adriatic extension, and kinematics of Neogene slip along the Saddle Mountains thrust

Gabriele M. Casale

A dissertation

submitted in partial fulfillment of the

requirements for the degree of

Doctor of Philosophy

University of Washington

2012

Reading Committee:

Darrel S. Cowan, Chair

Richard Bennett

Katharine Huntington

Program Authorized to Offer Degree:

Earth and Space Sciences

Abstract

The geometry and kinematics of map scale faults are the record of tectonic mountain building processes. This study focuses upon three distinct faults in three distinct orogens, the Alpi Apuane detachment in the Northern Apennines, the Mid-Bosnian Schist detachment in the internal Dinarides, and Saddle Mountains fault in eastern Washington.

Mountain building in the Central Mediterranean is controlled by convergence between the African and Eurasian continental plates, yet local kinematics and structural trends owe their genesis to a complicated interplay between discrete and often poorly defined continental and Oceanic fragments. The Peri-Adriatic sub-region of the Central Mediterranean is dominated by the Adria continental micro-plate; interaction between Adria and neighboring plates has given rise to the Eastern Alps, Apennines, Dinarides and Albanides. Of particular interest is a contrast in the role of extension along the convergent margins of the Adria plate. Along the western margin of Adria, subduction of Adria lithosphere beneath the Apennines has maintained syn-convergence extension from at least middle Miocene to the present; this process is manifested as a sustained cycle of burial, metamorphism, and subsequent exhumation along normal faults of Adria crust, and overlying fore-deep sediments. In the Dinarides, along the eastern margin of Adria, Jurassic-Eocene subduction of the distal oceanic portion of the Adria plate beneath Eurasia was concluded by collision and a change in subduction dynamics as the thick continental Adria lithosphere entered the subduction zone. In the first two chapters of this study I use field, microstructural, and thermochronometric techniques to determine the nature of shear zone tectonites and the thermal conditions during normal faulting in the Apennines, and the polarity and timing of slip along a detachment that cut to at least the middle crust in the internal Dinarides.

The third chapter of this study focuses upon elucidating the kinematics of fault slip using sub-surface seismic data within the Yakima fold-and-thrust belt in eastern Washington. In areas of active shortening, assessment of seismic hazards is difficult without a-priori knowledge of fault geometry. I determined geometric aspects of the Saddle Mountains anticline from a seismic reflection profile, and using kinematic forward modeling techniques, inverted for kinematically viable end member fault geometries representative of extant geometric models currently in use for seismic hazard assessment.

List of Figures

Acknowledgements ii

Chapter 1: Syn-convergence extension and mid-crustal exhumation in the Internal Dinarides; Bosnia-Herzegovina 1

1.1 Introduction 1

1.2 Geologic background 1

1.3 Results 5

1.3.1 Structure and kinematics 5

1.3.2 Thermochronology 8

1.4 Discussion 12

1.5 Conclusions 15

Chapter 2: Origin of the Calcare Cavernoso, implications for detachment slip at shallow crustal levels; Alpi Apuane metamorphic core comples, Italy 17

2.1 Introduction 17

2.1 Geologic background 17

2.2 Metamorphic and structural evolution 18

2.3 Origin of the Calcare Cavernoso 24

2.3.1 Sedimentary origin 25

2.3.2 Karstic origin 25

2.3.3 Tectonic origin 26

2.4 Analytical methods 27

2.5 Results 28

2.5.1 SEM, cathodoluminescence, and optical petrography 28

2.5.2 XRD 38

2.6 Discussion 40

2.6.1 Interpretation of petrographic observations 40
2.6.2 Stratigraphic relationship 43
2.6.3 T-P-t of faulting 44
2.7 Conclusions 46
Chapter 3: Kinematics of Neogene slip along the Saddle Mountains thrust 49
3.1 Introduction 49
3.2 Geologic background 49
3.3 Methods 53
3.4 Results 56
3.5 Discussion 59
3.5.1 Timing of anticlinal growth 59
3.5.2 Decollement slip and basement uplift 59
3.6 Conclusions 63
References cited 65

List of Figures

Regional geologic map of the Dinarides....3

Geologic map of the Mid-Bosnian Schist Mountains....4

Structural data....7

Exhumation model and cross section....10

Temperature-time paths....11

Geologic map of the Alpi Apuane....20

Stratigraphic column of the Alpi Apuane....21

Temperature-time paths of the Alpi Apuane....22

SEM photomicrographs....29

Reflected light photographs of fragmented clast....30

XPL photomicrograph of hydraulic fracture in limestone....31

XPL and CL of breccia clast in breccia....31

Reflected light image of handsample CV....33

CL photomicrograph of ghost grains and zoned cement....34

CL photomicrograph of mottled cement....35

Type II calcite twinning....37

XPL and CL photomicrograph of reworked vein....31

XRD results....39

Shaded relief map of the YFTB....51

SMA seismic section....54

Kinemtaic models....58

Kinematics of hanging wall folds....62

Acknowledgements

First and foremost I would like to thank my supervisor, Darrel Cowan, for his essential insight and guidance throughout each stage of my graduate work. Darrel has always encouraged and supported me to pursue my own interests and scientific goals, even when it has meant joining me in the field along contested boarders in precarious places. I would also like the thank Rick Bennett, who has inspired and motivated me from the beginning of my graduate work with his myriad and often dizzying interests, and commensurate energy. Many of the innumerable scientific conversations I shared with Rick and Darrel in the field are reflected in some form in the following chapters.

I am grateful to several individuals who have helped in a variety of ways towards the completion of this manuscript: I would like to thank Kate Huntington for her role on my supervisory committee, and always constructive and forthcoming feedback; Tom Pratt for his collaboration on the final chapter of this manuscript; Giancarlo Molli and Bruno Tomljenovic for hosting me in Italy and Croatia respectively; Peter Reiners and Paul O'Sullivan for thermochronometric work; Marijana Surkovic and Andy Gendaszek for assistance in the field; and my colleagues and fellow graduate students Eliza Nemser, Ryan Thress, Brenden Miller, Rachel Headley, Goran Buble, Karl Lang, Logan Chinn, for their camaraderie and intellectual support over the years; and Crystal Wilson for her thoughtful, and patient editing. Funding was provided by the ExxonMobil Corporation, the U.S. State Dept.'s Fullbright program, and the Department of Earth and Space Sciences at the University of Washington.

Lastly, completion of this work would not have been possible without the support of my family, who did not know what I was doing, but were nonetheless fairly confident that I could do it. In

particular, I owe an immense debt of gratitude to a certain Mina Luisa Casale, who executed flawless interference during the final stages of writing of this manuscript.

Chapter 1: Syn-convergence extension and mid-crustal exhumation in the Internal Dinarides; Bosnia-Herzegovina

1.1 Introduction

The MBSM are one of a series of crystalline orogen-parallel Paleozoic bodies in the Internal Dinarides, which form a constituent of the Dinaric Neotethys passive margin tectonostratigraphic nappe (Fig. 1.1). The MBSM are bounded along the NE and SE margins by an ENE dipping fault, which likely extends along the entire eastern margin where it is concealed by deformed Oligocene-Miocene sediments of the Zenica-Visoko-Sarajevo Basin (Fig. 1.2). Where the fault boundary is exposed, it has been mapped as a thrust fault (e.g., Vujnovic 1980; Jovanović et al., 1977) with a top-to-the-SW shear sense, consistent with the overall structural pattern of Dinaric fold-and-thrust belt architecture and previous interpretations of the MBSM as a fault bounded nappe. However, the stratigraphic juxtaposition across the fault is such that Cretaceous hanging-wall sedimentary rocks are in direct contact with Paleozoic basement; several kilometers of Mesozoic stratigraphic section are missing, a relationship that might be more readily associated with normal slip. We provide field observations and thermochronometric evidence that the MBSM bounding fault is a normal fault that penetrated to the middle crust, and that was active during the transition from oceanic to continental subduction along the internal Dinarides Neotethys margin.

1.2 Geologic background

The Dinarides are a southwest-vergent nappe-stack which can be roughly divided into three distinct tectonostratigraphic units; from structurally highest to lowest these include: the ophiolite nappe, the passive margin nappe, and the External Dinarides fold-and-thrust belt (Fig. 1.1). The latter fold-and-thrust belt is composed of Adria derived platform carbonates. This succession of

increasingly continental imbricated tectonostratigraphic nappes records late Jurassic to Eocene closure of the Meliata-Maliac-Vardar branch of the Neotethys ocean (Schmid et al., 2008). The transition from oceanic subduction to continental collision along the Adriatic portion of the Eurasian margin occurred in Paleogene time (Pamić 1993, Pamić and Jurković 2002; Ustaszewski et al., 2008) as recorded by biostratigraphically-determined depositional ages of passive margin clastics, platform carbonates, and syn-tectonic flysch (Tari Kovaćić and Mrinjek 1994). Closure of the Dinaric Neotethys was complete by early Miocene as is evident by capping of silicilastic flysch by Pannonian rift related sediments (Tari 2002). Encroachment of the subduction zone upon Adria continental lithosphere resulted in the cessation of deposition of clastic material of Nubian affinity upon the distal passive margin of Adria in the late Cretaceous (Pamić et al., 1998). A Paleocene hiatus of platform carbonate growth and a phase of emergence and karstification of the proximal portion of the Adria continental shelf (Vlahović et al., 2005) was coincident with migration of clastic deposition into the continental foreland (e.g. Tari 2002), evidence of uplift perhaps related to advancement of the flexural forebulge into the Adria foreland as a precursor to its entrance into the subduction margin. Minor carbonate platform deposition briefly resumed during early Eocene time in structural basins accompanied by trench related debris flows with final uplift and cessation in Oligocene time (Vlahović et al., 2005; Tari Kovaćić and Mrinjek 1994). Post collisional shortening resulted in the thrusting of Adria platform carbonates onto the Eurasian margin forming the External Dinarides fold-and-thrust belt (Pamić et al., 1998).

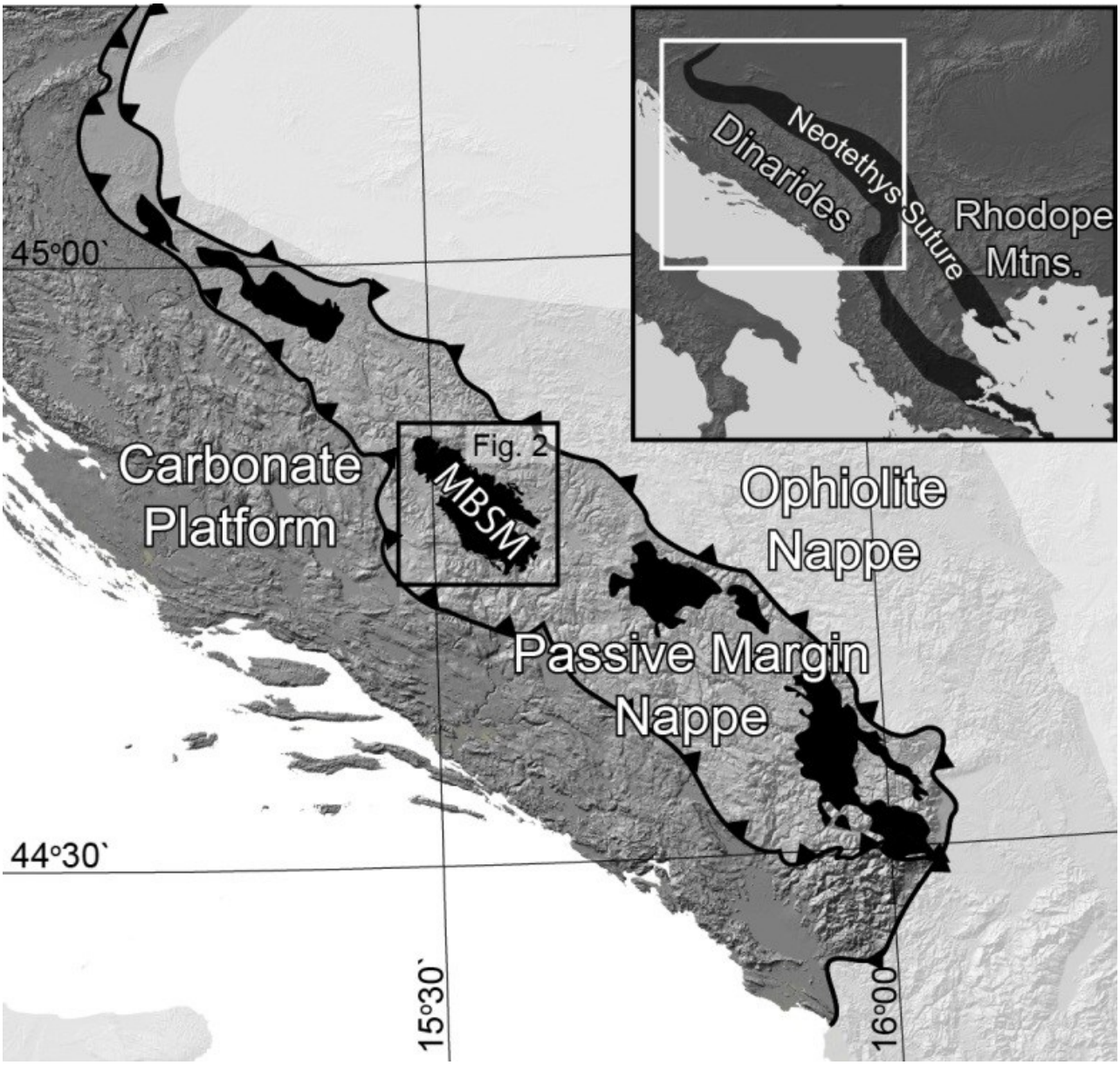

Figure 1.1. Regional geologic map of the Dinarides showing major tectonic boundaries between the ophilite nappe, passive margin nappe, and carbonate platform, the exhumed Adria passive margin basement (black), and the location of Fig. 1.2 (black box) (Simplified from: 1:500,000 geologic maps of Yugoslavia sheets Zagreb, Sarajevo, Novi Sad, Dubrovnik, Beograd, Skopije, Federal Geological Institute, 1970; Ustaszewski et al., 2010; Pamic et al., 2000).

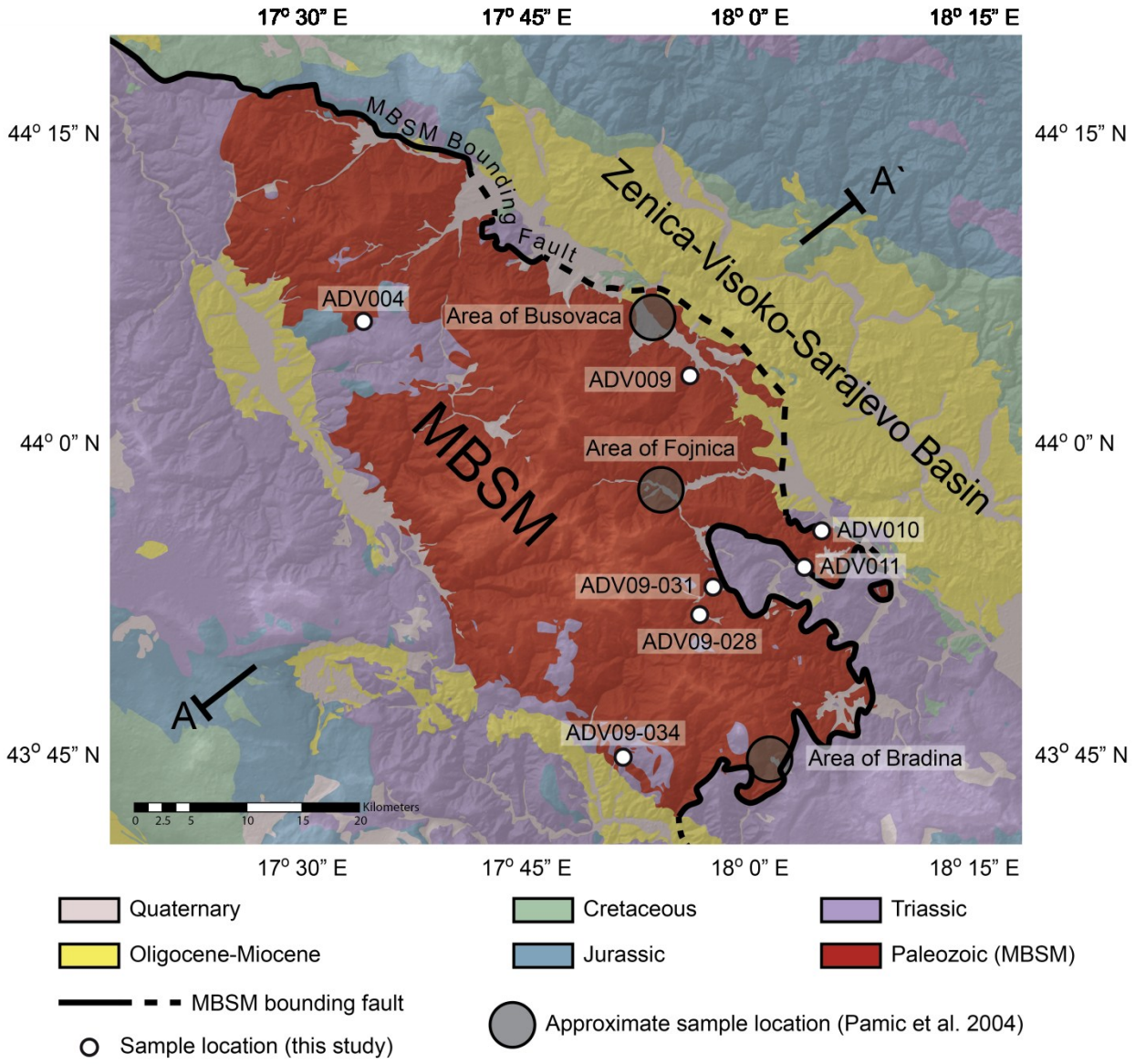

Figure 1.2. Geologic map of the Mid Bosnian Schist Mountains simplified from 1:100,000 geologic maps of Yugoslavia with sample numbers and locations, end-points of the section trace for Fig. 1.3, and approximate locations for dates from Pamić et al., (2004).

A similar record of collision can be traced along the Tethys suture from the Alps through Anatolia, yet interpretation of collisional and post collisional tectonics differs greatly along strike. Southeast of the Dinarides, in the Rhodope Mountains, closure of the Tethys basin and entrance of continental lithosphere into the convergent margin resulted in regional extension, which included high-angle graben-bounding normal faults, extensive mid-crustal exhumation along low-angle normal faults, and regional volcanism (Burchfiel et al., 2008 and refs therein). The Dinaric portion of the Tethys suture is similarly marked by exhumed crystalline basement and volcanism (Pamić 1993; Pamić et al., 2000, Kovác et al., 2007); however, these Internal Dinaride crystalline bodies have previously been interpreted as allocthonous Paleozoic nappes emplaced during collisional mountain building along thrust faults, rather than exhumed along extensional faults (Pamić et al., 1998; Pamić et al., 2004).

1.3 Results

1.3.1 Structure and kinematics

The goal of the field component of this study was to determine the shear sense across the fault bounding the eastern margin of the MBSM. The interpretation of the MBSM as a fault bounded allochthonous nappe requires a top-to-the-SW shear-sense across the bounding fault, whereas exhumation along a normal fault predicts a top-to-the-NE sense-of-shear. We collected field measurements of shear-sense indicators to distinguish between the two opposing kinematic interpretations and determine the emplacement mechanism of the MBSM mid-crustal rocks in their current upper crustal position.

Riedel composite structures and asymmetric folds record kinematic shear-sense, and Mode I fractures record maximum principal stretching direction. We follow the nomenclature of an

idealized Riedel composite structure, which includes: a shear plane (Y), synthetic high and low-angle normal faults (R and R` respectively), and a foliation plane (P) antithetic to R. In a lower hemisphere projection the slip vector is located at the intersection between the girdle containing the four Riedel planes and the Y plane, with a slip-sense similar to the R faults. The distribution of asymmetric fold axes can be used to determine shear sense and slip vector orientation of a shear zone. In an ideal monoclinic shear zone, fold-axes of clockwise and anticlockwise polarity are distributed on opposite sides of a girdle defining the Y plane. The slip vector lies on the Y plane at the boundary between populations of axes of opposing polarity, and relative shear sense is in agreement with rotational polarity (Cowan and Brandon, 1994). Poles to Mode I fractures are parallel to the maximum principal stretching direction.

Field measurements consistently show top-to-the NE kinematic shear sense, with minor discrepancy in slip vector orientation between Riedel composite structures and asymmetric folds within the shear zone (Fig. 1.3). The slip vector discrepancy is likely due to the influence of local strain variation being exaggerated by limited sampling opportunities. Despite variation between datasets, the proximity between the best-fit pole to the Riedel Y plane (Fig. 1.3B, Pr) and the pole to the calculated shear plane from the asymmetric fold axes (Fig. 1.3B, Pf) indicates consistency between datasets. The poles to mode 1 fractures (Fig. 1.3C) cluster in the NE and SW quadrants in a lower hemisphere projection, indicating NE-SW orientation of the principal stretching direction. The general pattern of top-to-the-NE shear sense and NE-SW maximum stretching supports our interpretation that the MBSM bounding fault is a NE dipping normal fault and implies extensional exhumation.

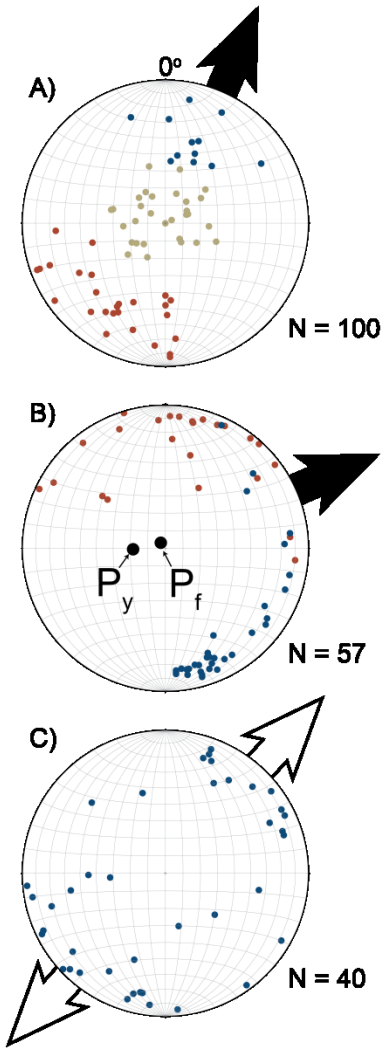

Figure 1.3. Lower hemisphere equal area projections of structural data. 3A: poles to Riedel composite structures, including P (blue), Y (tan), and R (red), black arrow indicated the approximate orientation of hanging-wall motion with respect to the foot-wall. 3B: Asymmetric fold axes, folds with clockwise rotation (red) and anticlockwise rotation (blue). Black arrow indicates the sense of motion of the hanging-wall with respect to the foot-wall. 3C: Poles to mode 1 fractures, open arrows indicate the orientation of the principal stretching direction.

1.3.2 Thermochronology

Previous thermochrometric studies of the MBSM were limited to one ^{40}K-^{40}Ar study of whole-rock and single mineral measurements (Pamić et al., 2004). For that study, cooling ages fell into four distinct age groups: early Permian, late Cretaceous, early Eocene, and late Eocene, which were interpreted as distinct tectonic events regionally correlated to events recorded elsewhere in the Balkans and Eastern Alps. With the exception of one Paleozoic ^{40}K-^{40}Ar hornblende age (247.0 ± 9.5 Ma) all of the mono-mineralic ages from Pamić et al. (2004) were in the youngest group contemporaneous with Eocene Dinaric Neotethys closure. These were interpreted as a heating event resulting from post-orogenic strike slip faulting.

Measurement of multiple thermochronologic systems is useful in determining the thermal path during exhumation (e.g. Foster and John 1999; Brichau et al., 2006; Fellin et al., 2007). We complement published medium temperature ages with low-temperature measurements of zircon fission track (FT), and U-Th/He in zircon and apatite in the metamorphic core (Fig. 1.4). Our results show a pattern similar to previously published mono-mineralic measurements with Eocene zircon FT and U-Th/He ages, younger late Miocene ages for apatite U-Th/He, and one upper Jurassic zircon FT age. The relatively short interval between closure of hornblende ^{40}K-^{40}Ar (500 ^{o}C,) (Harrison and McDougall 1981) and zircon He (180 ^{o}C) (Reiners 2005) indicates a phase of rapid cooling during Eocene time. The distribution of ages is too complex for a single one dimensional cooling model with some low-temperature ages predating higher temperature ages; however, a clear younging-to-the-NE pattern becomes apparent by projecting sample locations on a SW-NE cross sectional trace (Fig. 1.4). We spatially divide ages into three groups defined by reset ages in zircon FT and hornblende ^{40}K-^{40}Ar, which yield distinct permissible one-dimensional cooling paths with younger cooling from increasing depths from SW to NE

(Fig. 1.5). In the southwestern most group (yellow) zircon FT is not reset, indicating shallow burial to temperatures no greater than 240 ^{o}C (Brandon et al., 1998) since late Jurassic time. The central group (orange) was buried to between 240 ^{o}C and 500 ^{o}C degrees as indicated by reset zircon FT and un-reset hornblende ^{40}K-^{40}Ar respectively. In the northeastern-most group all thermochronmetric systems are reset by burial to at least 500 ^{o}C (reset hornblende ^{40}K-^{40}Ar) until Eocene cooling. Our kinematic interpretation is consistent with the spatial distribution of thermochronologic ages, and suggests that the metamorphic core is the exhumed footwall cutoff of the MBSM bounding fault. From SW to NE the pre-exhumational burial temperature increases, and single mineral cooling ages decrease. Normal dip-slip along a northeast dipping fault, as depicted in Fig. 1.4, predicts the progressive down dip exhumation of deeper rocks.

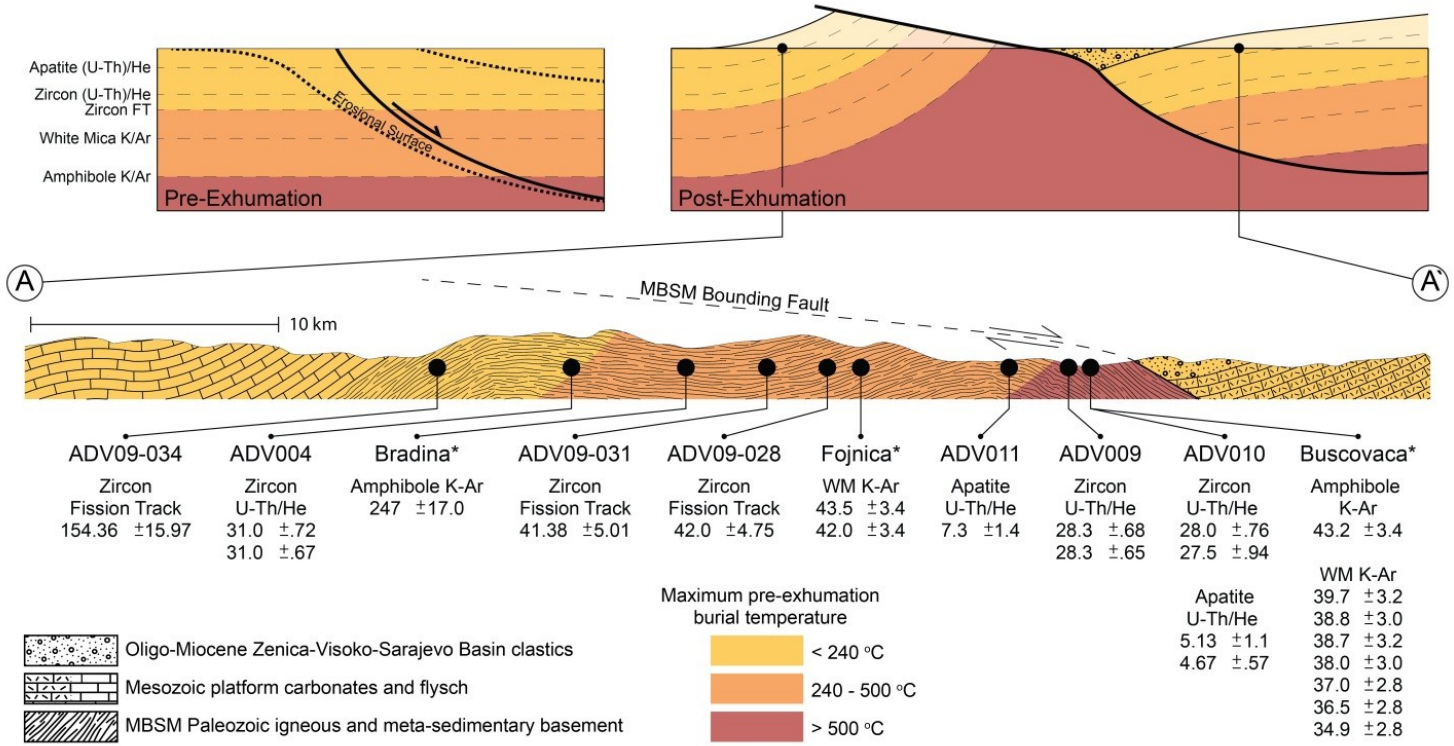

Figure 1.4. Schematic cross sections across the MBSM depicting the pre-exhumational geometry and future erosional surface (upper left), post-exhumational geometry (upper right) and sample locations projected horizontally and perpendicular to the section trace (center, see Fig. 1.2 for locations). Colors correspond to areas grouped by pre-exhumational maximum temperature, and correlate to the cooling paths in Fig. 1.5. These groups include: maximum temperature below zircon FT (240 ^{o}C) (yellow), between zircon fission track (240 ^{o}C) and hornblende ^{40}K-^{40}Ar (500 ^{o}C) (orange), and above hornblende ^{40}K-^{40}Ar (500 ^{o}C) (red). *Results from Pamić et al., (2004). In the pre-exhumation model the NE dipping MBSM bounding fault cuts progressively down such that post-exhumation the surface profile of the exhumed foot-wall shows a lateral progression in progressively higher temperature rocks from SW to NE. The total amount and distribution of post exhumational erosion is unknown but likely accounts for at least several kilometers of denudation.

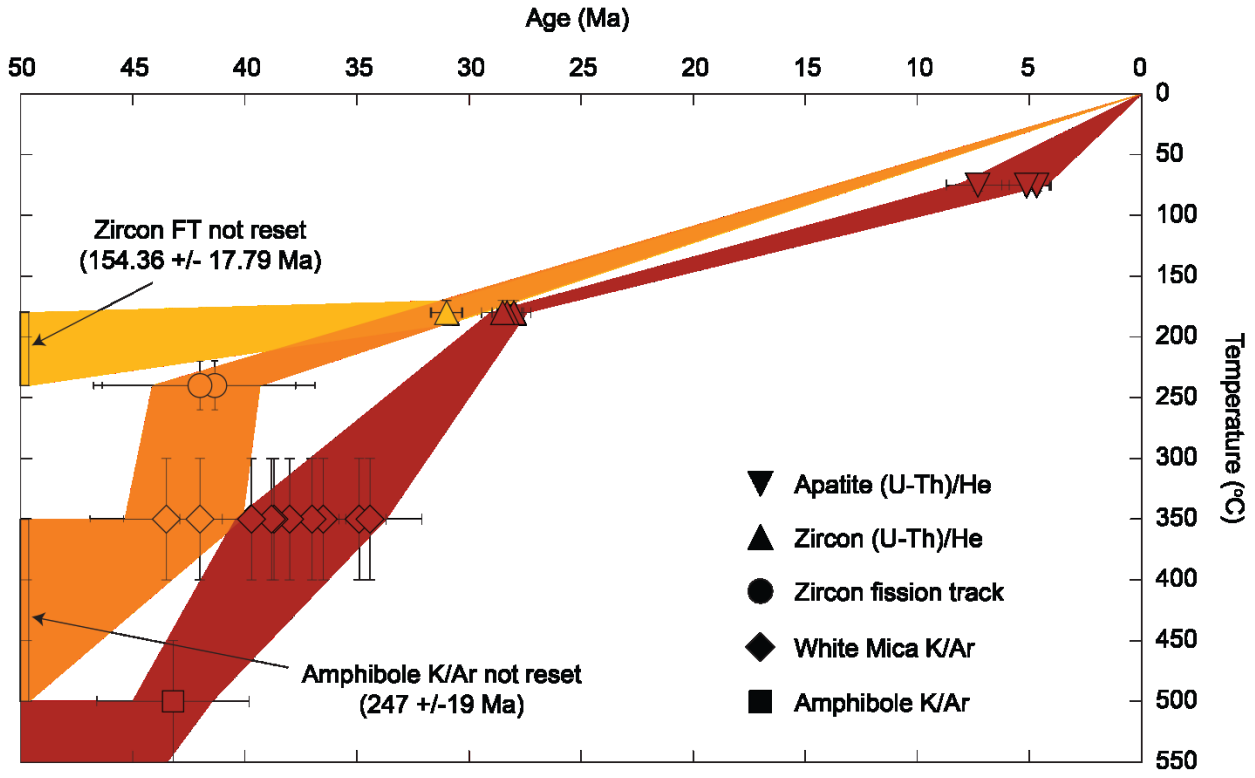

Figure 1.5. Temperature-time graph of thermochronologic results from this study with dates from Pamić et al. (2004), and estimated cooling paths of thermal-geographic groups with color designations as in Fig. 1.4. Cooling paths determined by closure temperatures of ~75 °C for apatite U-Th/He (Wolf et al., 1998), ~180 °C for zircon U-Th/He (Reiners 2005), ~240 °C for zircon FT (Brandon et al., 1998), ~350 °C for Muscovite ^{40}K-^{40}Ar (Hames and Bowring 1994), and ~500 °C for hornblende ^{40}K-^{40}Ar (Harrison et al., 1981).

Whole-rock ages are problematic due to uncertainty in the contribution of various thermochronometric systems within a sample. However, the progressively younger-to-the-northeast pattern of whole-rock ages reported in Pamić et al. (2004) is consistent with our pre-exhumational geometry and kinematic exhumation interpretation. Due to lateral variation in the exhumed geothermal gradient we suggest that diversity in reported whole-rock ages perhaps reflects the varying contribution of reset Eocene ages and Paleozoic-Mesozoic growth ages rather than true ages of distinct tectonic events. Notably, the youngest whole-rock ages are similar to mono-mineralic ages in the northeast where pre-Eocene exhumation temperatures

exceeded the closure temperature of the highest temperature ^{40}K-^{40}Ar thermochronometric system (hornblende ^{40}K-^{40}Ar).

1.4 Discussion

Our field kinematic observations and thermochronologic data provide, for the first time, evidence of significant spatially concentrated extension contemporaneous with the onset of continental collision along the paleogeographic Adria-Eurasia margin. Although quantification of fault throw or pitch are hampered by several factors, including syn- and post-exhumational erosion and doming, the SW-NE lateral extent of exposed mid-crustal foot wall suggests approximately 35 km of slip. An assumed ~30 ^{o}C/km geothermal gradient indicates ~10-15 km of 'throw' exposed in the footwall; we estimate the fault dip as roughly 15-25^{o} NE. This NE dipping fault is overlain by sediments of the Zenica-Visoko-Sarajevo basin which we consider a half graben. Thus the MBSM may be regarded as a Cordilleran type metamorphic core complex exhumed from mid-crustal depths along a low-angle normal fault.

While the extent and timing of collision-related extension elsewhere in the Internal Dinarides is unknown, previous studies have described extension related to Miocene intermontane basin development (Mandić et al., 2009), Pliocene inversion tectonics (Tomljenović and Csontos 2001; Saftić et al. 2003), and one study of core complex type exhumation along the Sava depression, a subsidiary of the Pannonian system of basins (Ustaszewski et al., 2010). Intermontane basin development has been attributed to late orogenic extension associated with strike slip faulting, or opening of the Pannonian basin (Illić and Neubauer, 2005). The observed Miocene mid-crustal exhumation in the Sava depression was interpreted as part of the extensional processes related to the Carpathian roll-back driven opening of the Pannonian Basin (Ustaszewski et al., 2010). Extension and exhumation of the MBSM described here appears to predate these other observed

extensional processes suggesting that it is related to a different tectonic event. Several other Paleozoic complexes are present and situated along the paleogeographic Adria-Eurasia margin. Although thermochronologic data from these complexes is sparse or non-existent, their shared geometric similarities with the MBSM invite speculative interpretation of their origin via a common geodynamic process, and suggest the possibility of regional extension.

Disagreement exists regarding the nature and timing of deformation in the Dinarides. Some authors conclude mountain building by Oligocene time (e.g. Vlahović et al., 2005; Pamić et al., 1998) and attribute Neogene deformation to post orogenic strike-slip faulting (e.g. Picha 2002; Mandić et al., 2009). However, nano-fossil assemblages in deformed tectonic flysch indicate that thrusting was active until at least middle Miocene time (Mikes et al., 2008; de Capoa et al., 1995), and geodetically derived surface velocities provide evidence for ongoing shortening, perhaps involving subduction of Adria mantle lithosphere beneath the Dinarides (Bennett et al., 2008). Sustained shortening throughout the Neogene indicates that exhumation of the MBSM core complex was synchronous with mountain building, rather than post-orogenic collapse.

The syn-collisional extension we observe in the MBSM shares a timing relationship and tectonic setting with extension observed along the Tethys margin in the southern Balkan extensional system. In the Rhodope Mountains, collision was immediately followed by extension and mid-crustal exhumation and volcanism along the paleogeographic margin (Burchfiel et al., 2008); Eocene collision in the Internal Dinarides was followed by MBSM exhumation 43-28 Ma (this study) and emplacement of granitoids and latites in the Durmitor passive margin nappe (Pamić et al., 2000; Pamić 1993). Similarly, in both regions collision and extension accompanied, rather than post-dated, ongoing shortening and orogenesis.

The underlying mechanism driving post, late, or syn-orogenic extension is debated contentiously, and has variously been attributed to slab detachment (Wortel and Spakman 2000), slab roll-back (Royden, 1993), excess gravitational potential energy of an over-thickened wedge (Platt et al., 1989; Rey et al., 2001), or post-orogenic gravitational collapse (Malavieille et al., 1990). However, not all of these processes are mutually exclusive; they may act in concert, or give way to one-another over time. Gravitational collapse has been cited as driving early extension along the southern Eurasian margin (Burchfiel et al., 2008), and is predicted by a change in subduction dynamics. Subsequent sustained extension, southward migration of shortening and extension, and a steeply dipping slab revealed in tomographic images across the Aegean suggests slab roll-back drives present geodetically observed extension there (Bijwaard et al., 1998; Jolivet and Brun, 2010).

The contemporaneity of MBSM core complex exhumation and cessation of flysch deposition in marine trenches along the suture zone suggests a link between the transition from oceanic to continental subduction and the onset of extension. However, the pattern of sustained extension migrating in the wake of similarly-migrating compressional and volcanic belts observed in the Hellenic system is absent in the Dinarides. Existing tomographic images across the Dinarides reveal a shallowly dipping subducted slab roughly twice the width of the External Dinarides fold-and-thrust-belt (Piromallo and Morelli, 2003; Bennett et al., 2008). No estimates of total shortening in the Dinarides exist; the length of the imaged slab (~160 km) is likely insufficient to account for the total length of lithosphere consumed during emplacement of the passive margin and ophiolite tectonostratigraphic nappes. The geometry and length of the extant slab implies removal of some amount of the subducted Dinaric Neotethys lithospheric mantle. Stein and Sella (2006) suggested that the subducted lithospheric slab was removed by a NW migrating tear

initiated in the SE Dinarides at 30Ma, reaching the Eastern Alps in the NW by 15 Ma, and similar models have been proposed to account for extension and volcanism further north along the Periadriatic lineament (von Blanckenburg and Davies 1995, 1996, von Blanckenburg et al., 1998, and others).

Wortel and Spakman (2000) provide a conceptual model that demonstrates that collision may initiate slab tear, causing uplift, a significant tectonic stress perturbation, and an extensional response in the over-riding orogenic wedge. The timing of Sella and Stein's (2006) tear model is relative and not determined by local geologic evidence; the 43-28 Ma extensional exhumation of the MBSM and emplacement of granitoids and latites correlate with Wortel and Spakman's (2000) model; this correlation suggests that tear propagation in the Dinarides may have initiated during Eocene time, concurrent with slab tear in along the Periadriatic lineament. Further support for Eocene breakoff may be inferred from geodesy and seismic imaging; continued subduction of Adria mantle lithosphere since Eocene time at the geodetically imaged rate of ~4 mm/yr is consistent with the current 160 km length of slab as revealed by tomographic images (Bennett et al., 2008).

1.5 Conclusions

Map patterns, thermochronometric measurements, and field kinematic observations indicate that the MBSM is a Cordilleran-type metamorphic core complex exhumed between 43-28 Ma along a low-angle normal fault. Consistent top-to-the NE sense of hanging-wall displacement observed in shear zone kinematic shear sense indicators, supported by a SW to NE progression in cooling ages, indicates exhumation of the MBSM along a normal fault dipping approximately 15-30^{o} to the NE with approximately 35 km of slip. Concentrated pre-Pannonian (Miocene) extension pervading to at least mid-crustal levels has not been previously documented in the Dinarides, and

the spatial extent of related extension is unknown. However, several other Paleozoic bodies share geometric and paleogeographic similarities with the MBSM metamorphic core complex; these similarities suggest that extension is perhaps widespread. Extension in the Dinarides may be the crustal response to a changing tectonic setting during the transition from oceanic to continental subduction and closure of the Tethys ocean basin. Our interpretation agrees with regional spatio-temporal patterns observed throughout the neighboring southern Balkan region. A limited length of tomographically imaged mantle lithosphere beneath the Dinarides is consistent with Eocene slab breakoff as a possible mechanism for extensional deformation and exhumation of the MBSM.

Chapter 2: Origin of the Calcare Cavernoso, implications for detachment slip at shallow crustal levels; Alpi Apuane metamorphic core comples, Italy

2.1 Introduction

The purpose of this study is to provide primary textural observations and interpretations of microscale fabrics within the CV, a rock of disputed origin found along a detachment exhuming mid-crustal rocks. Textures within tectonized fault rock provide a record of the kinematics and conditions during faulting. Inferences regarding the tectonic evolution of the Alpi Apuane metamorphic core complex in the Northern Apennines, have largely relied upon observations of hanging-wall and foot-wall rocks away from the fault zone because the CV, which occupies the fault zone, has been interpreted as the result of a number of different tectonic and non-tectonic processes. Our observations bear directly on a number of outstanding question regional and tectonic questions, such as the role of fluids and the P-T condition under which detachment faulting may occur, and the role of evaporites in the tectonic evolution of the Northern Apennines hinterland extensional belt.

2.1 Geologic background

The Northern Apennines are an east-directed stack of imbricate nappes that make up the accretionary prism above the western margin of the subducting Adria micro-plate. Counter-clockwise rotation of the subduction margin is attributed to roll-back of the steeply dipping Adria slab (Malinverno and Ryan, 1986; Dewey, 1988; Royden, 1993; Faccenna et al., 1996; Jolivet et al., 1998; Brunet et al., 2000; Rosenbaum and Lister., 2004), which has resulted in the Oligocene to present migration of the Apennine foreland fold-and-thrust belt from the eastern margin of Corsica to its present location (Jolivet et al., 1998). Extension has closely followed migration of

the convergent margin and resulted in hinterland crustal attenuation that is characterized by basin-and-range type graben-bounding normal faults, and low-angle normal faults that exhume mid-crustal metamorphic rocks.

Accretion in the foreland operates in concert with extrusion in the hinterland. Adria continental crust and fore-deep flysch are accreted along thrust faults and ultimately extruded along normal faults in the hinterland. The progression from shortening in the accretionary foreland to extensional extrusion in the hinterland is accommodated in part by re-activation of decollements as detachment horizons. The tectonostratigraphic position occupied by the CV is an example of one of these thrust faults reactivated as a normal fault during extensional mid-crustal exhumation of the Alpi Apuane metamorphic core complex (Carmignani and Kligfield, 1990; Boccaletti and Sani, 1998).

2.2 Metamorphic and structural evolution

A series of deeply exhumed metamorphic complexes occupy the hinterland extensional belt in the Northern Apennines; the Alpi Apuane is the largest and most deeply exhumed of these complexes. Kinematic and petrologic observations within the Alpi Apuane metamorphic core have formed the basis of our understanding of dynamic processes in the deepest part of the Apennines orogenic wedge, and record the transition from shortening and burial to uplift and exhumation (Carmignani and Kligfield, 1990, Carmignani et al., 1994). The Alpi Apuane metamorphic core is composed of two main tectonostratigraphic units, the structurally higher Massa unit to the west, and the Apuane unit to the east (Figs. 2.1 & 2.2). Accretion of the Alpi Apuane core prior to metamorphism is dated to 34-27 Ma by preserved fossil assemblages in the upper-most stratigraphic section of the Apuane unit (PseudoMacigno fm.) (Dallan-Nardi, 1977; Carmignani and Giglia, 1978; Montanari and Rossi, 1983) (Fig 3). Different peak P-T conditions

are recorded in the Massa and Apuane units (0.6-0.8 GPa and 420-500 ^{o}C, and 0.4-0.6 GPa and 350-420 ^{o}C respectively; Di Pisa et al., 1985; Franceschelli et al., 1986; Jolivet et al., 1998; Molli et al., 2000a, 2000b, 2002). However, in both the Apuane and Massa units peak conditions were reached simultaneously at 27.0-23.8 Ma (Kligfield et al., 1986).

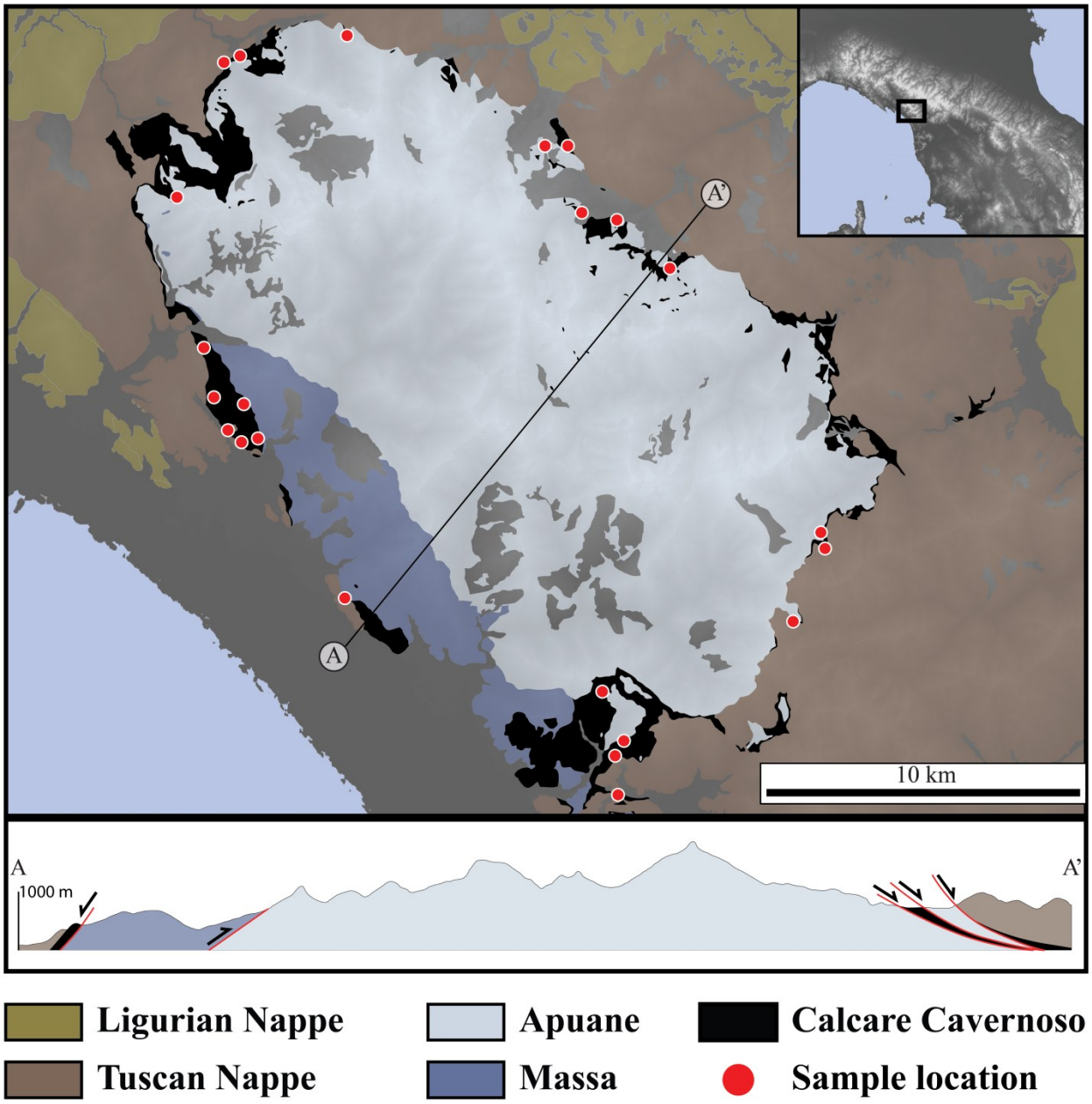

Figure 2.1. Geologic map of the Alpi Apuane metamorphic core complex showing sample locations simplified from Carmignani et al. (2000), and schematic cross section simplified from Carmignani and Kligfield (1990). The map and cross section depict the structurally controlled distribution of the Calcare Cavernoso; along the tectonic margin of the Alpi Apuane between the Tuscan Nappe and Apuane and Massa metamorphic units, or along faults near the margin of the metamorphic core.

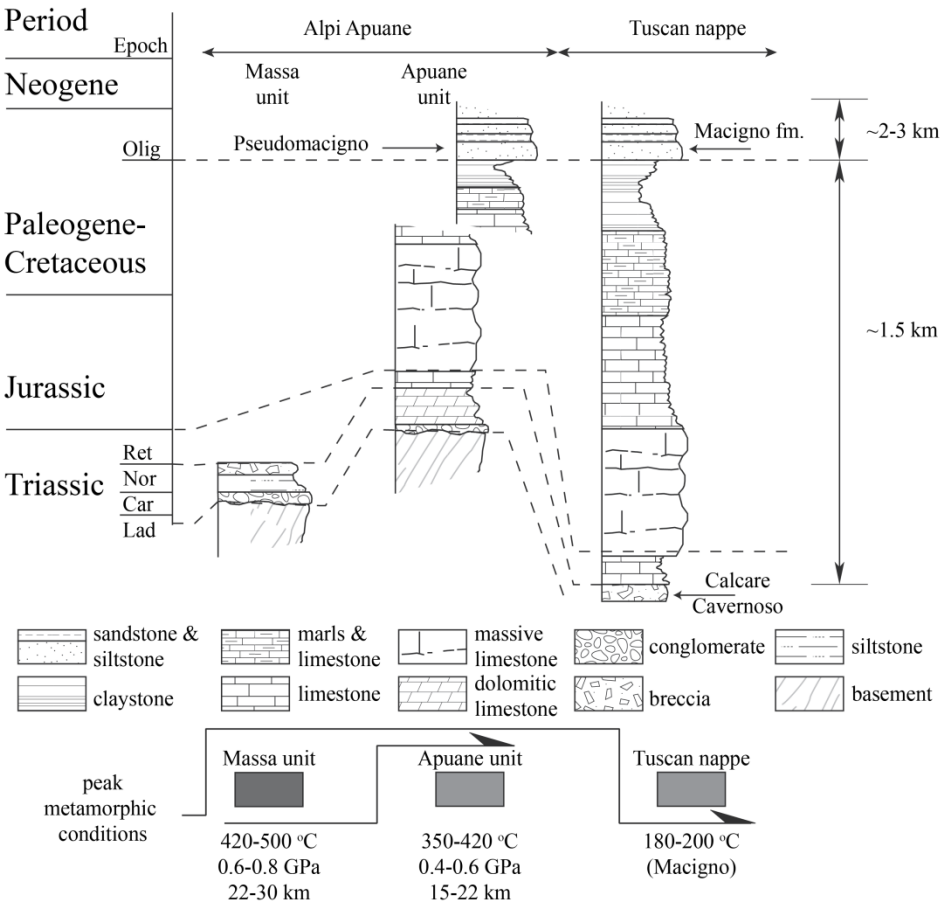

Figure 2.2. Stratigraphic column of the Alpi Apuane metamorphic units and the Tuscan nappe (from Fellin et al., 2007, after Decandia et al., 1968, and Carmignani et al., 2000). The Tuscan nappe and Apuane units are rough stratigraphic equivalents composed of Adria derived carbonates overlain by siliclastic sediments (Macigno fm. and Pseudomacigno fm., respectively) deposited in the Apennines fore-deep. The CV is commonly assigned to the Triassic base of the Tuscan nappe.

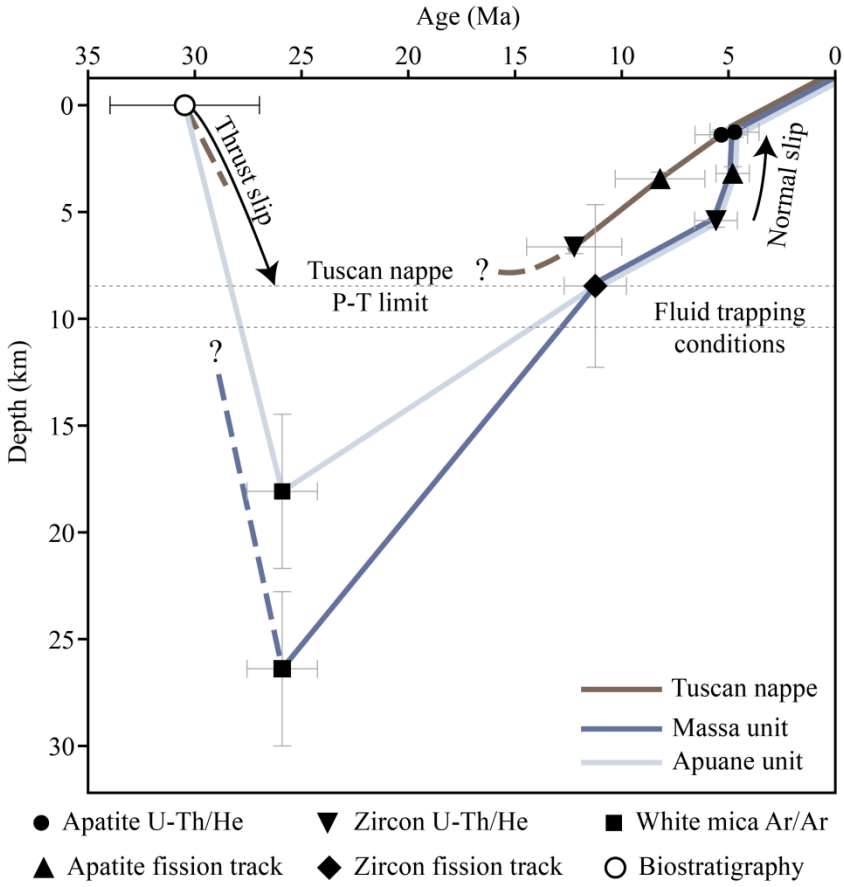

Figure 2.3. Burial paths of the Alpi Apuane metamorphic core (Apuane and Massa units) and the structurally overlying Tuscan nappe (modified from Fellin et al., 2007) as determined by biostratigraphic ages (Dallan-Nardi, 1977; Carmignani and Giglia, 1978; Montanari and Rossi, 1983), Ar/Ar (Kligfield et al., 1986), zircon and apatite fission track and U-Th/He data (Fellin et al., 2007), and peak P-T data from the metamorphic core (Di Pisa et al., 1985, Franceschelli et al., 1986, Jolivet et al., 1998, Molli et al., 2000a, 2000b, 2002a). Peak P-T conditions of the Tuscan nappe is limited by detrital (un-reset) ages of zircon fission track in the Macigno formation. Fluid trapping conditions were estimated from fluid inclusions in quartz and calcite veins located in the shear zone (Hodgkins and Stewart, 1994). Arrows correspond to the timing and depth of slip along the Tuscan nappe basal shear-zone related to burial and exhumation of the metamorphic core, and correspond to phases of known differential heating or cooling between the Tuscan nappe and Alpi Apuane metamorphic units. Depths estimates from closure temperatures are from Fellin et al. (2011) and are based on one-dimensional steady state solution (see Reiners and Brandon, 2006), this thermal model includes advection, which accounts for the slight variation in the depth to closure between foot-wall and hanging-wall thermochronometers.

The thermochronometric record of the exhumation of the Alpi Apuane metamorphic core includes several distinct cooling phases. From peak metamorphic conditions the Apuane and

Massa units cooled at slightly different rates, simultaneously reaching the closure temperature of zircon fission track (~240 ^{o}C, ~8 km depth) at 10-13 Ma (Fig. 2.3). Subsequently, both metamorphic units cooled together at a reduced rate, equivalent to an exhumation rate of ~.7 mm/yr, punctuated only briefly during Pliocene time (4-6 Ma) with an exhumation rate of ~1.4 mm/yr between the closure temperatures of zircon U-Th/He (~180 ^{o}C, ~5.5 km depth), and apatite U-Th/He (80-100 ^{o}C, ~1.9 km depth) (Balestrieri et al., 2003; Fellin et al., 2007; Balestrieri et al., 2011).

Uplift and exhumation of the Alpi Apuane metamorphic core can be divided into two general phases. Late-stage (<13 Ma) upper-crustal exhumation of the metarmophic core is attributed to low-angle normal faulting (Carmignani and Kligfield, 1990; Carmignani et al., 1994; Balestrieri et al., 2003; Jolivet et al., 1998; Fellin et al., 2007; Balestrieri et al., 2011, and others) accompanied by high-angle normal faulting in both the hanging-wall and foot-wall (Carmignani and Klifgield, 1990; Ottri and Molli, 2000) and graben infilling (Bernini et al., 1990; Mauffret et al., 1999). Early-stage (>13 Ma) uplift was accommodated either by pervasive ductile thinning due to extension in the middle crust (Carmignani et al., 1978; Carmignani and Giglia, 1979; Carmignani and Kligfield 1990; Carosi et al., 1996) or under-plating and mid-crustal thickening (Boccaletti et al., 1983; Carosi et al., 2002, 2004). In either case most authors agree that exhumation from peak metamorphic conditions (15-30 km) to upper crustal conditions (~9 km) occurred prior to 10-13 Ma (Fellin et al., 2007).

The hanging-wall of the Alpi Apuane detachment is composed of the Tuscan nappe, which is overlain by the Ligurian ophiolite nappe (Fig. 2.2). Like the Alpi Apuane metamorphic rocks, the Ligurian and Tuscan nappes were accreted in the Apennines foreland. The Tuscan nappe is composed of a ~1.5 km thick Triassic-Eocene succession of carbonates overlain by the 2-3 km

siliciclastic Macingo fm. (Costa et al., 1992) (Fig. 2.3). Stratigraphic equivalency between the Macino fm., and the Pseudomacigno fm. of the Apuane unit is evidence of the contemporaneous accretion of these two units in the Apennines foreland. However, unlike the greenschist facies Apuane unit, the anchizonal Tuscan nappe was not deeply buried. Estimates of peak burial conditions in the Tuscan Nappe are determined by thermochronometric studies which bear reset U-Th/He and detrital fission track ages in zircon (Fellin et al., 2007; Bernet et. al., 2009) corresponding to a maximum burial temperature of ~200^{o}C (Reiners and Brandon, 2006) (FIG. 3). Recognition of a gap in metamorphic grade across the Alpi Apuane detachment led early authors to conclude that this boundary was a tectonic contact associated with emplacement of low grade rocks of the Tuscan nappe (Merla, 1951; Elter et al., 1960; Gianni et al, 1962; Baldacci et al., 1967). The observation that the Apuane and Massa mid-crustal rocks were exhumed along a low-angle normal fault led to the characterization of the Alpi Apuane as a cordilleran type metamorphic core complex (Carmignani and Kligfield, 1990).

2.3 Origin of the Calcare Cavernoso

Despite the modern consensus that the margin of the Alpi Apuane metamorphic core is a tectonic boundary, tectonic fabric is rarely observed even where this boundary is well exposed. Instead, the fault zone is occupied by a polymictic carbonate breccia (CV). Rocks sharing the distinct texture of angular vuggs in a fine carbonate matrix of the CV have been observed elsewhere in the Alps and Apennines (locally referred to as rauhwacken, carniole, cornieules, cargneules), and attributed to a variety of tectonic or sedimentary processes. Genetic interpretations of these various carbonate breccias categorically include: a sedimentary origin, a product of karstification, a tectonic origin, or of mixed origin (Alberto et al, 2007, and references within).

2.3.1 Sedimentary origin

Field and microstructural observations led some authors to conclude that the CV was a sedimentary breccia (Dallan-Nardi and Nardi, 1973; Patacca et. al., 1973; Federici and Raggi, 1974; Dallan-Nardi, 1979; Sani, 1985; Abbate and Bruni, 1987; Coli, 1989). These observations include: (1) a sedimentary basal contact with the underlying metamorphic core and sedimentary structures such as grading, stratified laminar bedding, and cross-bedding (e.g. Dallan-Nardi and Nardi, 1973, Federici and Raggi, 1974, Sani, 1985, Fazzouli et al., 1994), and (2) the presence of Orbulina Universa (Dallan-Nardi, 1979; Sani, 1985), a Miocene-present species of marine foraminifera. Geometric measurements of sedimentary features are scarce; however Dallan-Nardi and Nardi (1973) provide field photographs of some of these sedimentary structures in an analogous polymictic breccia in the Monte Pisani to the SE.

A sedimentary origin of the CV would hold particular significance because the unit contains metamorphic clasts derived from underlying Alpi Apuane metasediments (Federici and Raggi, 1974; Sani, 1985). The presence of these clasts in a sedimentary rock would require exhumation and erosion of the metamorphic core prior to emplacement of the overlying Tuscan nappe. If the CV has a sedimentary origin, the emplacement of the Tuscan nappe must be younger than the biostratigraphically determined Miocene depositional age of the CV.

2.3.2 Karstic origin

Several authors have hypothesized that the CV and similar rocks observed elsewhere are the result of in-situ karstic reworking. Alberto et al., (2007) proposed that the Pseudocarniole in the western Alps, a lithologic unit that bears many textural similarities with the CV, is a product of dissolution and collapse. In their model, volume reduction via dissolution of underlying gypsum and anhydrite by hydrothermal fluid ascension causes brecciation by gravity collapse of the

overlying carbonates. Similar models for the development of the CV in the Apennines have been proposed that include dissolution cycles of gypsum and anhydrite (Merla, 1951; Gandin et al., 2000), and evidence of cyclical hydration, dissolution, and precipitation of evaporites is preserved in the Burano fm. (Lugli, 2002). Hydrothermal circulation through evaporites is active in numerous hydrothermal springs present to the east of the Apuane region within the Tuscan and Ligurian nappes (e.g. Monsummano, Montecatini, Bagni di Lucca, Gallicano, Barga, Torrite, Pieve di Fasciana, Equi terme, and Monzone springs). Dissolved sulfur and δ^2H and $\delta^{18}O$ ratios of thermal waters from the Bagni di Lucca (some 10 km to the SE of the Alpi Apuane metamorphic core) indicate deep circulation of meteoric water and dissolution of underlying evaporites (Boschetti et al., 2005). Moreover, physical analogies within the Apennines support the possibility that the CV has been re-worked in-situ. In the Frasassi caves in the Marche region, abundant gypsum precipitation is attributed to oxidation of groundwater H_2S derived from dissolution of anhydrite at depth (Galdenzi and Marouka, 2003). Elsewhere in the Apennines, clast-in-matrix fabrics somewhat resembling the CV have been observed in fluvial-karst deposits (e.g. Mugnano cave, see Martini, 2011). Based on field observations and carbon and oxygen isotopic values, Feroni et al., (1976) similarly concluded that the ambiguous texture of the CV was locally the result of karstic reworking in the presence of meteoric water.

2.3.3 Tectonic origin

A tectonic origin of the CV is primarily compelled by the structural relationship between the Tuscan Nappe, and Alpi Apuane metamorphic core. The proposed Miocene deposition of the CV post-dates the Oligocene emplacement of the overlying Tuscan Nappe, and is contemporaneous with deep burial of the Apuane and Massa units. This sequence of events is problematic because the CV sits below the Tuscan nappe, and includes clasts from the metamorphic core, which could

not have been exposed to erosion. This problem is resolved if instead the CV was developed as a tectonic breccia along a detachment, and the presence of both metamorphic and sedimentary clasts is explained as the result of in-situ tectonic mixing of the foot-wall and hanging-wall rocks (Carmignani and Kligfield, 1990). However, this hypothesis has not been thus far supported by kinematic data measured in the field.

2.4 Analytical methods

We collected samples of CV from 23 locations distributed along the entire margin of the Alpi Apuane metamorphic core (Fig. 2.1). We prepared standard 30 μm-thick thin-sections for use in petrographic, cathodoluminescence, and scanning electron microscope analysis. For X-ray diffractometry, matrix and clast material was carefully powdered directly from cut surfaces using a 0.5 mm diameter drill. Relict clast material was sampled from angular vugs to determine lithological control on this differential erosion characteristic of the CV.

Polished thin sections were analyzed in plane and crossed polarized light with a standard petrographic microscope. Cathodoluminescence observations were made on a Relion cathodoluminescent stage under approximately 10-2 Torr vacuum, and 10 keV accelerating voltage focused beam. SEM observations and measurements of four samples were made using a FEI Quanta 200 scanning electron microscope. Phase compositions were measured by energy dispersive spectrometry using an EDAX Genesis XM calibrated to Smithsonian National Museum of Natural History (NMNH) mineral standards and with a 5 μm spot size. XRD measurements were made on a Shimadzu 6000 X-ray diffractometer with 2θ values ranging from 5-80^{o}. SEM analyses were conducted at the William C. and Ruth A. Dewel Microscopy Facility, XRD, CL, and optical microscopy analyses were conducted at the Appalachian State University department of Geology.

2.5 Results

2.5.1 SEM, cathodoluminescence, and optical petrography

We observe the CV to be polymictic in all samples except one. Although clast content is heterogeneous and widely variable between samples, clast types are restricted to rock types found in direct contact with the CV. In many samples clast populations include both Alpi Apuane metamorphic lower-plate and Tuscan Nappe upper-plate sedimentary rock types. Lower-plate foliated siliciclastic and mica-rich clasts are easily identifiable, and in some cases upper-plate carbonate clasts are distinguishable by preserved fragile microbial laminations. Clast lithologies readily attributable to the upper-plate are exclusively fine grained calcite and dolomite. In most cases uniformly carbonate samples are composed of only upper-plate clasts. Lower plate lithologies are significantly more variable and include foliated quartz rich meta-sandstones, phyllitic schists, and marbles. Similar lower- and upper-plate lithologies (e.g. Macigno and Pseudomacigno fms.) are distinguishable at high magnification with the SEM (Figs. 4a, 4b). Pseudomacigno clasts are foliated with biotite, muscovite, or chlorite in crystallographic preferred orientation and often contain small (<5 μm) authigenic garnets; these metamorphic phases are present only as detrital grains in the sedimentary Macigno fm. The presence of these metamorphic minerals and textures indicates that these clasts are derived from lower-plate metamorphic lithologies. In a few locations, clasts composed of un-twinned quartz grains with non-undulatory extinction contain small (<5 μm) idiomorphic gypsum crystals (Fig. 2.4c). We interpret these undeformed gypsum-bearing quartz grains as re-worked authigenic vein fill rather than re-worked detrital or metamorphic grains due to the idomorphic solid inclusion morphology, and absence of sub-grains.

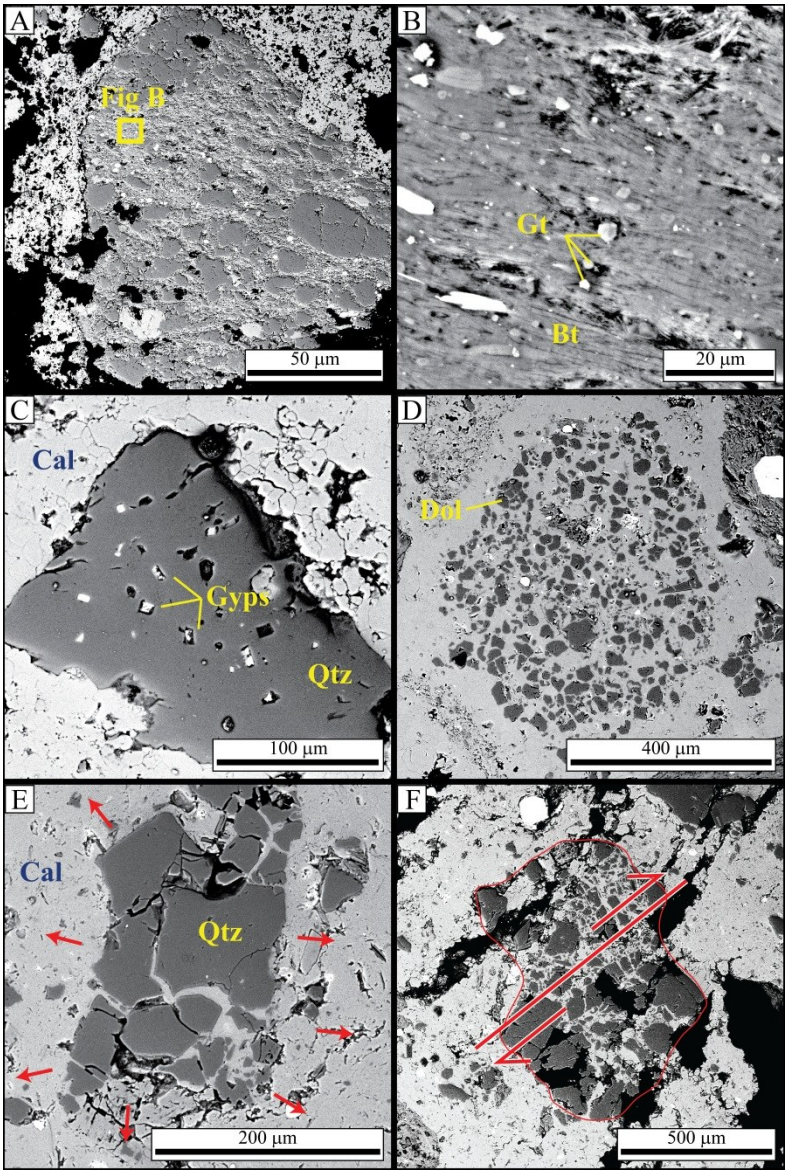

Figure 2.4. SEM micrographs of various fabrics in the CV. A) foliated Pseudomacigno metasandstone in calcite matrix. B) Foliated fabric within Pseudomacino clast (A) showing garnet and biotite metamorphic phases useful in distinguishing foot-wall derived metasedimentary clasts from hanging-wall sedimentary stratigraphic equivalent units. C) Relict quartz vein material reworked as a clast, and containing gypsum euhedra. D) Relict dolomite clasts undergoing de-dolomitization by replacement with calcite. E) Jigsaw pattern brecciation in a quartz clasts. F) Reworking of previously cemented breccia clast showing right lateral offset.

Re-working and in-situ comminution of clasts is commonly preserved. Comminution is preserved as groupings of angular lithoclasts clearly attributable to a single original clast. Clast fragments are arranged alternatively as elongate configurations of fragments (Fig. 2.5), or more

closely grouped in local jigsaw-puzzle patterns limited to single clasts (Figs. 2.4e, 1.4f). In many locations, primary or secondary jigsaw puzzle brecciation is pervasive. In secondary jigsaw-puzzle brecciation, angular clasts are composed of breccia (Fig. 2.6). Primary jigsaw-breccias typically occurs in previously undeformed upper-plate carbonate rocks. Several samples comprise lithologically heterogeneous breccia clasts that are texturally identical to the matrix but distinguishable by variation in cement luminescence; we interpret these clasts as reworked cemented breccia (Fig. 2.7).

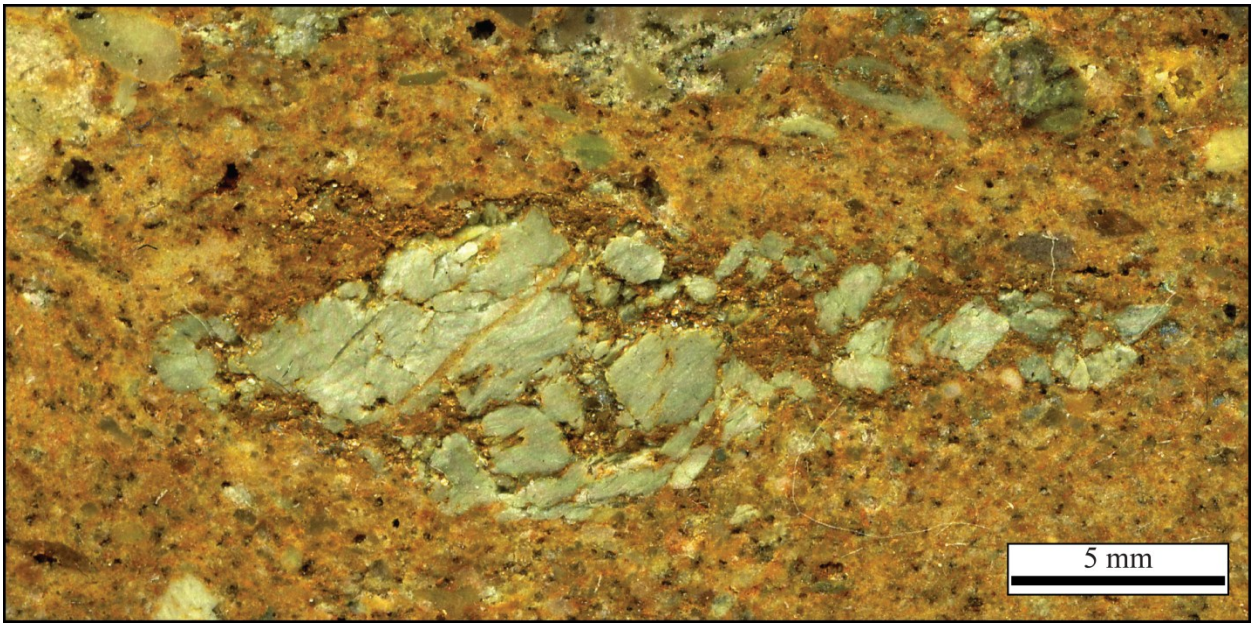

Figure 2.5. Reflected light image of a fragmented foliated foot-wall metasedimentary clasts. Light colored elongate clasts is composed of foot-wall metamorphic calc-silicate and is surrounded by a fine grained cataclastic matrix composed of a mixture of hanging-wall and foot-wall derived fragments. Fracturing of the calc-silicate clasts is accompanied by translation of fragments and infilling of interstitial space by fine grained cataclastic matrix material. This type of brittle fracture suggests cataclastic flow at shallow crustal conditions.

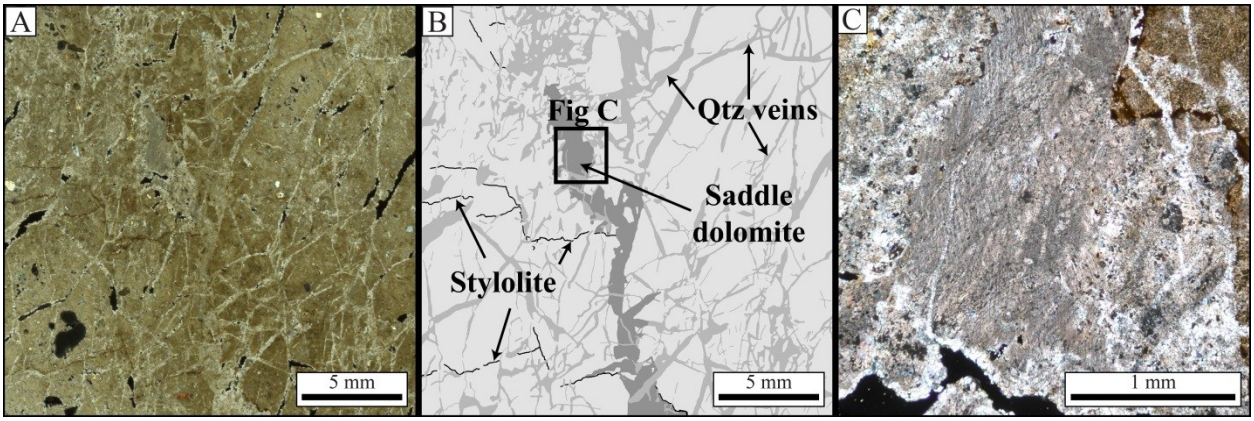

Figure 2.6. A) Cross-polarized light image of jigsaw pattern brecciation of cohesive cataclastic matrix by at least two phases of hydraulic fracture, including an intermediate phase of dissolution along stylolitic surfaces. B) Schematic trace of vein and stylolite patterns from (A). Early vein infilling by saddle dolomite is evidence of elevated fluid temperatures. The saddle dolomite vein terminates at stylolitic surfaces. Both stylolites and saddle dolomite are cut by a later phase of pervasive hydraulic fracturing and infilling by calcite. C) Saddle dolomite is distinguished by characteristic curved twin boundaries. Cross cutting by of the early cataclastic matrix and saddle dolomite by later calcite veining is apparent in the upper right hand corner of the image.

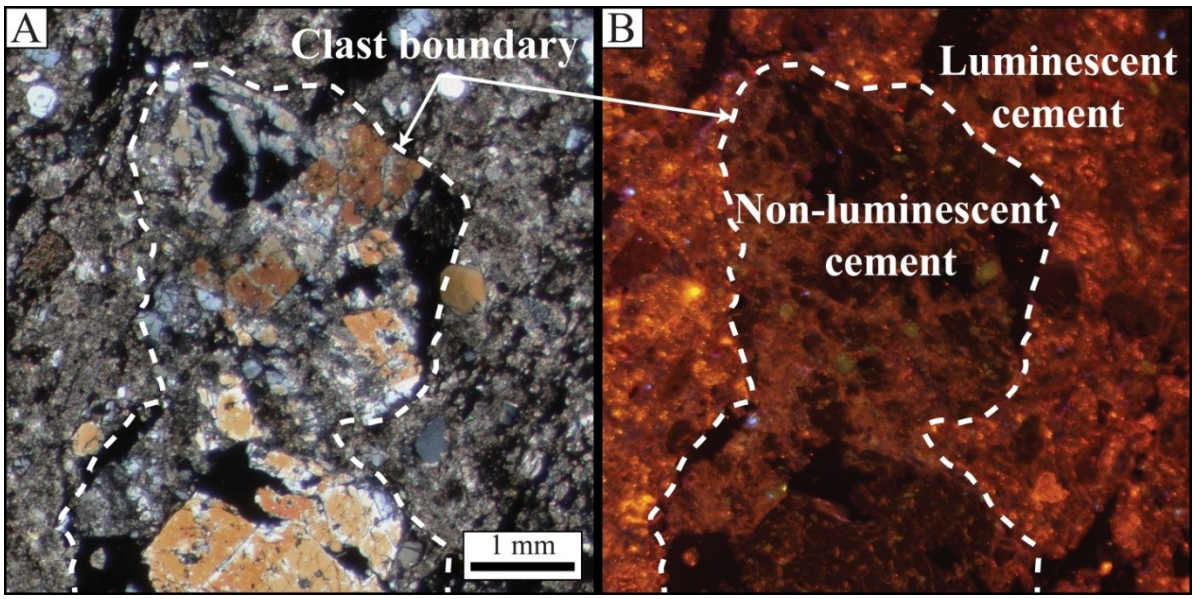

Figure 2.7. A) Crossed-polarized light photomicrograph of a clast of cohesive breccia (outlined by white dashed line) reworked as a clast in a cataclastic matrix. B) CL image of (A) showing the contrast in luminescence between the low-luminescent matrix within the reworked breccia clast, and the younger luminescent cataclastic matrix. Reworking of cemented breccia as clasts within breccia is evidence of in-situ tectonic re-working, and multiple phases of brecciation and cementation.

Texturally the CV ranges significantly between locations, from non-foliated course angular clast supported breccia to foliated fine grained matrix supported cataclasite or gouge with sub-rounded clasts (Fig. 2.8). Matrix content ranges from 0%, to nearly 100%, and a first order inverse relationship exists between clast angularity and matrix content. Clast angularity varies to a lesser degree with clast lithology; phyllitic schists are generally well-rounded whereas both foot-wall and hanging-wall carbonates range from angular to sub-rounded. In general both clast angularity and size are variable within individual samples. We did not observe ghost fabrics in large angular clasts, a feature diagnostic of diagenetic infilling of pore space between detrital grains (Boggs and Krinsley, 2006). Small (<50 μm) ghost grains of well-rounded matrix clasts are observed in idomorphic zoned dolomite euhedra within the matrix of foliated samples (Fig. 2.9). We interpret these grains as late-stage cementation and infilling as described below. In the only monomict sample, no matrix is present; instead interstitial space between angular clasts is occupied by authigenic sparry calcite and several voids are partly filled with drusy-sparite. In matrix-supported samples the matrix is composed of a mixture of fine-grained calcite and silicate fragments. Foliation is defined by spaced pressure solution cleavage or preferred long-axis orientation of elongate grains (Figs. 8b, 8c), and in a few cases is accompanied by pressure shadows filled with fibrous calcite.

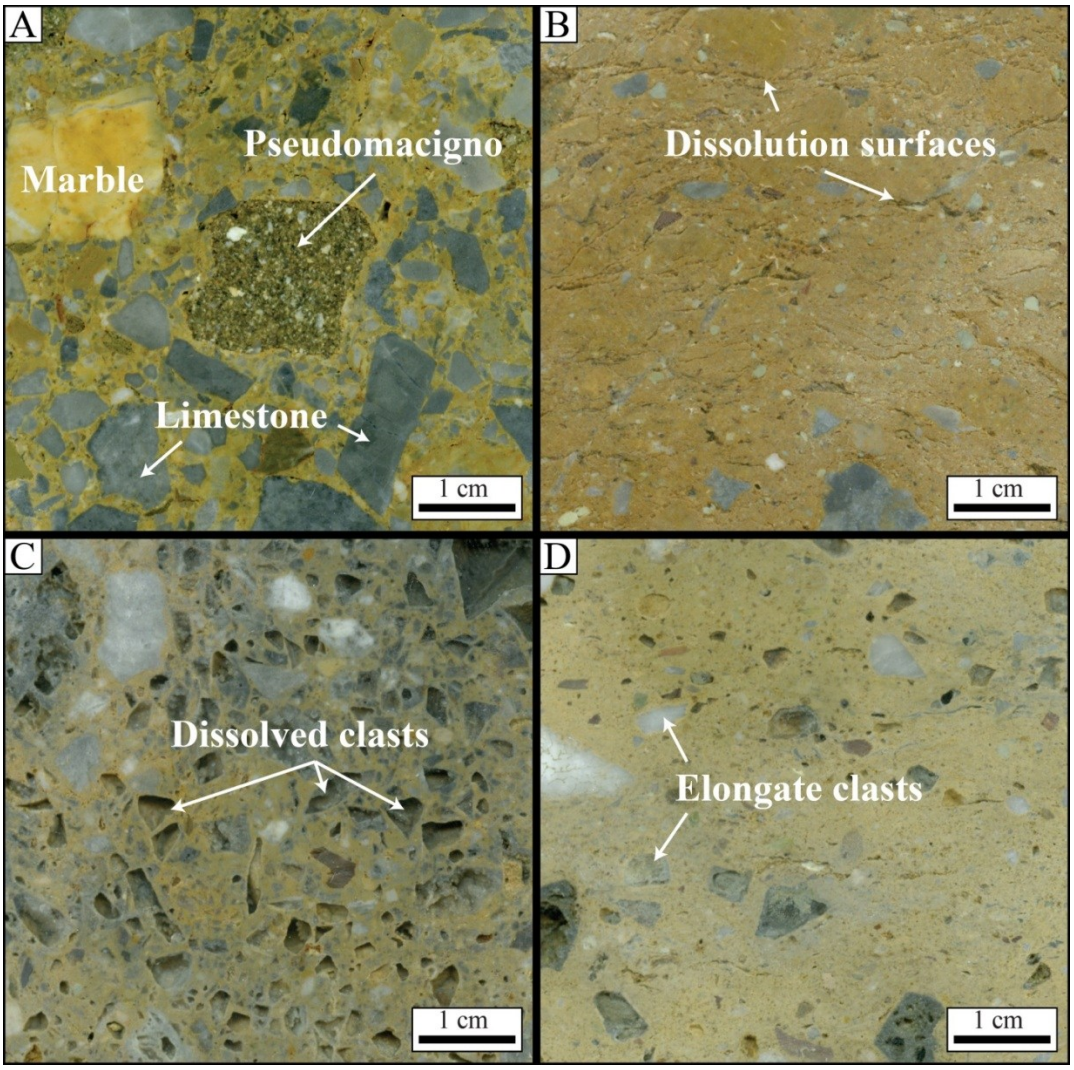

Figure 2.8. Reflected light images of polished hand samples showing textural heterogeneity between various CV samples. Figure (A) depicts clear clast heterogeneity including marble and pseudomacigno clasts from the metamorphic foot-wall and various limestone rock-types from the hanging-wall. Figure (B) exhibits a pervasive undulatory planar foliation defined by dissolution surfaces. Figure (C) bears the distinct 'cavernoso' texture of angular vugs in matrix, the result of dissolution of chemically susceptible clasts. The preserved clast casts indicated that prior to dissolution this rock type likely resembled the angular clast in matrix texture observed in figure (A). Figure (D) shows a weak foliation defined by the preferred orientation of elongate sub-rounded clasts-in-matrix in cataclasite. Images (A) and (C) depict breccia members of the CV, containing greater than 30% clast material. Images (B) and (D) are matrix supported cataclasite with less than 30% clast material.

In CL the fine grained matrix in both matrix- and clast-supported polymict samples has a mottled orange luminescent texture of varying intensity (Fig. 2.10). The variable matrix luminescence contrasts to generally more homogenous or organized orange or red luminescence in carbonate clasts. We interpret this mottled texture as the result of mixing of comminuted clasts and deformed calcite cement. In most samples, the youngest cement has an irregular fibrous texture filling interstitial spaces between the matrix grains and along boundaries of larger clasts. The youngest cements often display a geometric zoned epitaxial pattern, occasionally including calcite or dolomite euhedra (Fig. 2.9). These cements exhibit bright alternating bands of dark to bright orange-red luminescence. This pattern is typical of carbonate precipitation during changing fluid conditions, and perhaps related to the transition from phreatic to vadose conditions (Boggs and Krinsley, 2006).

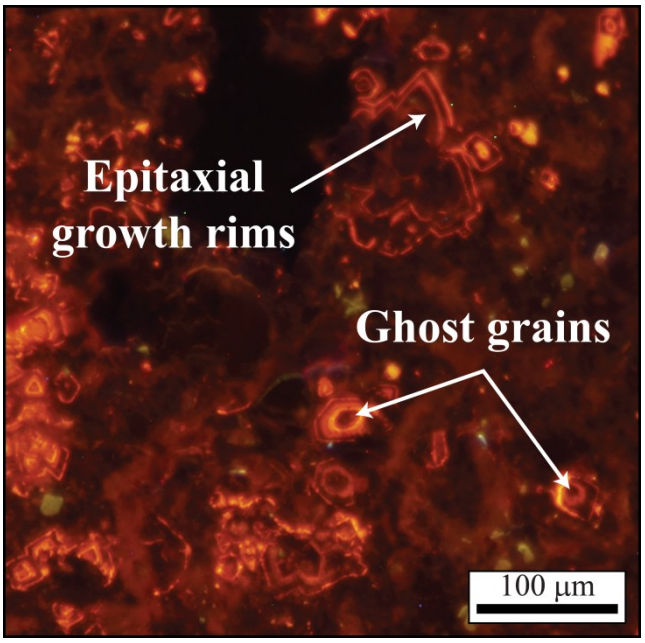

Figure 2.9. CL photomicrograph showing ghost grains and epitaxial zonation, defined by alternating bands of varying luminescence intensity, in late stage cements. Envelopment by idomorphic calcite or dolomite is only observed around ghost grains in fine-grained matrix material. This pattern of epitaxial growth rims is often associated with diagenetic cementation of clastic material (Boggs and Krinsley, 2006). Typically diagenetic cements have low luminosity, this CL image was taken with a 6 minute exposure and low gain (ISO 300).

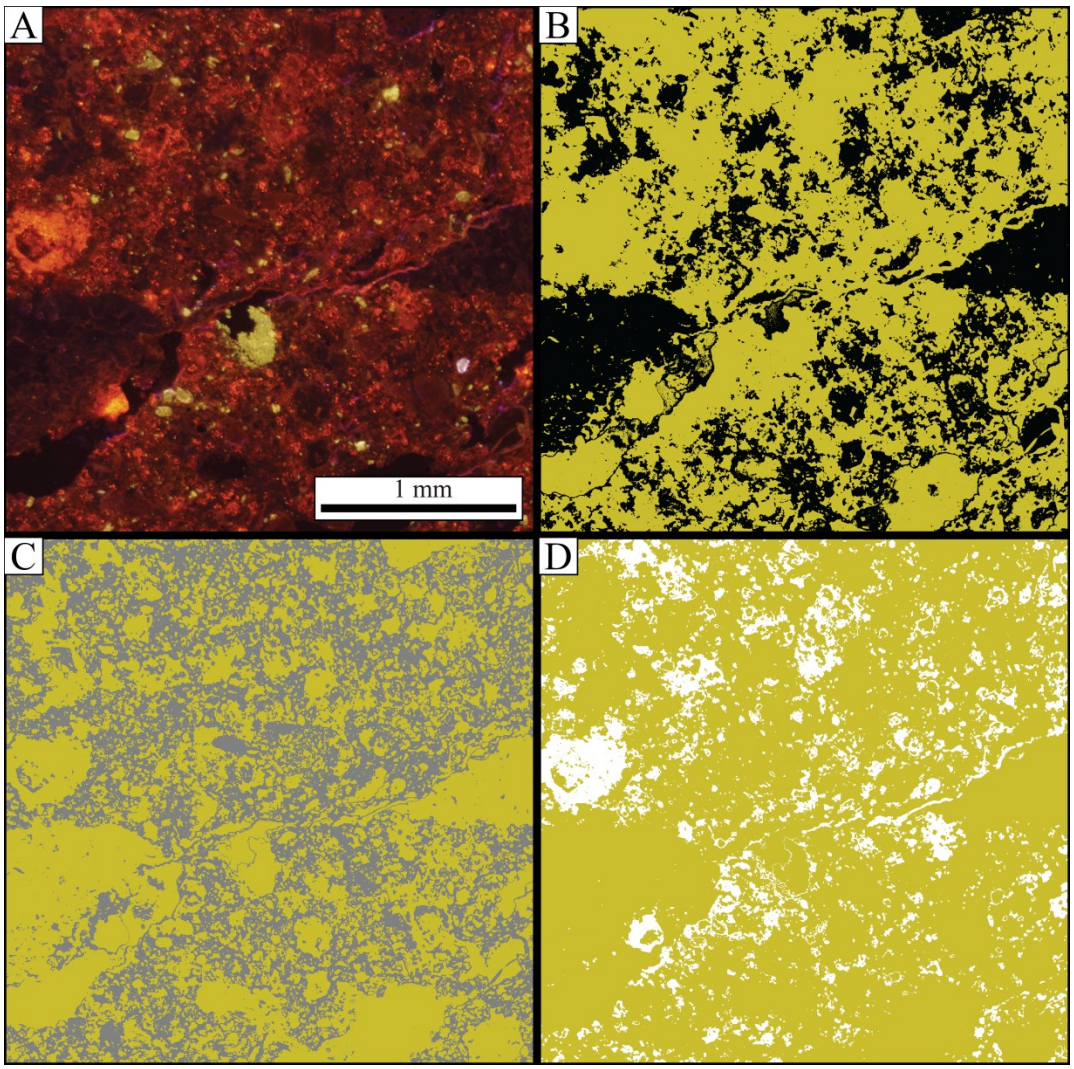

Figure 2.10. (A) CL photomicrograph of cataclastic matrix showing carbonate precipitation from at least three fluid compositions. Three distinct phases are apparent by varying luminescence intensity. Carbonate phases are aliased into three discrete bins by grey-scale intensity, and include dark (B, black), intermediate (C, grey), and bright (D, white). This depiction of intensity distribution demonstrates the disorganization of the various carbonates, and suggests that precipitation was accompanied by progressive cataclasis. Bins were chosen based on breaks in the grey-scale pixel distribution curve and do not necessarily have any physical implications.

Veining and dissolution surfaces are common in micro-scale. Calcite vein fill is often sparitic or fine grained; fibrous vein fill is only observed in one sample and is largely contained within a single clast. Multiple generations of calcite veins are present in most samples, with veins alternatively cross-cutting matrix-clast boundaries, bending along clast margins, or contained within clasts and terminating at the clast matrix interface. In foliated samples, sparite filled veins are often cut by, or refracted along dissolution surfaces. In veins cross-cutting both clast and matrix, the calcite infill is commonly syntaxial and non-luminescent, and is therefore likely precipitated following fracture-opening in oxidizing meteoric fluids (Boggs and Krinsley, 2006). Twinning in calcite vein fill is common and restricted to type I and II twins (narrow straight twins < 1 μm wide, and straight tabular twins > 1 μm wide, respectively) (Passchier and Trouw, 2005) (Fig. 2.11). In several samples, saddle dolomite occurs as either relatively thick (3-5 mm) veins (Fig. 2.6) or angular clasts (Fig. 2.12). Notably, quartz veins are non-existent, and authigenic quartz is only observed in a few locations as isolated euhedral grains. Stylolitic surfaces are commonly less than 1 cm in length and account for only small amounts of dissolution (<1 mm). These dissolution surfaces are not observed to cut late-stage non-luminescent veins. Local dissolution surfaces are also observed along indentations between soluble grains; however, their relationship to late stage veining is not possible to determine in our samples.

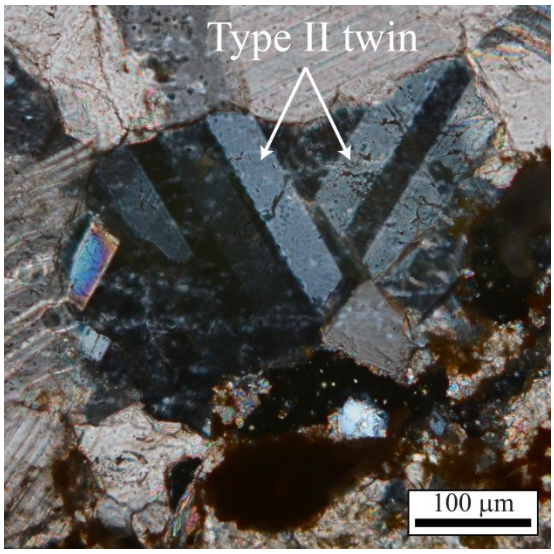

Figure 2.11. Example of type II twinning in a calcite vein cross-cutting cataclastic matrix. Type II twinning in calcite is characterized by tabular twins greater than 1 μm in width, and is evidence of strain accumulation at temperatures between 200-300 ^{o}C (Passchier and Trouw, 2005 and references therein).

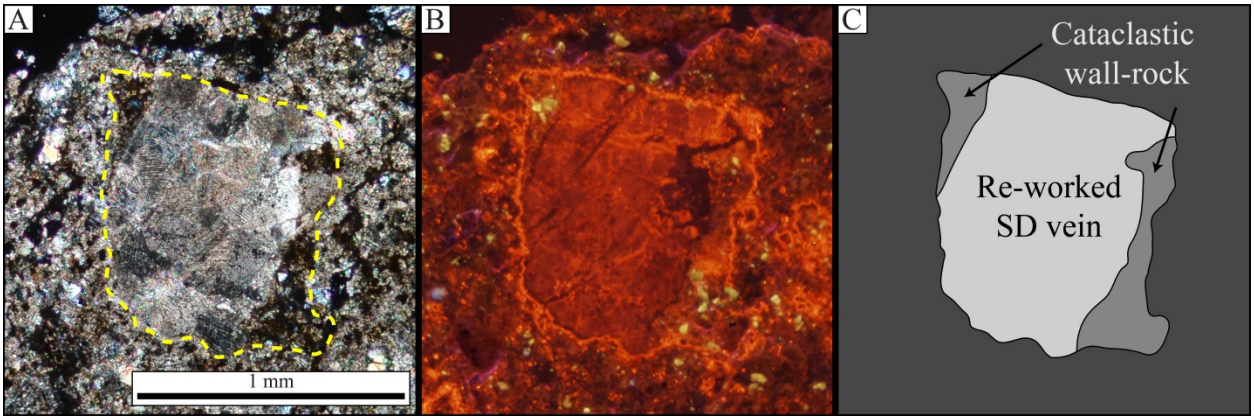

Figure 2.12. Photomicrograph (A) and CL image (B) of a reworked saddle dolomite vein in matrix as a clast in cataclasite as depicted schematically in (C). Boundaries of the reworked clast are outlined in the dashed yellow line in (A) and appear as a bright red luminescent rim in (B). The presence of cataclastic wall-rock within the reworked clasts indicates progressive reworking of a cemented cataclastic matrix, which had previously undergone hydraulic fracturing by fluids at elevated temperatures.

2.5.2 XRD

Relict clast material from angular vugs in two samples contains dolomite; in another sample this same relict material is primarily calcite, which is perhaps replacement calcite from primary dolomite (Fig. 2.13 bottom) (a process that we observed in SEM) (Fig. 2.4d). In either case our findings support the conclusion by previous authors that the characteristic angular vugs in the CV are due to differential weathering of poorly cemented carbonate clasts (e.g. Carter et al., 1994).

In all samples the dominant matrix phase is composed of calcite. Variously, dolomite, quartz, albite, chlorite, muscovite, biotite, rutile, and hematite are present as secondary phases unevenly distributed among samples. Notably, gypsum, anhydrite, and magnesite are below the detection limit of XRD, and with the exception of very rare inclusions of gypsum in quartz, we did not observed these phases in our petrologic or SEM analyses (Fig. 2.13).

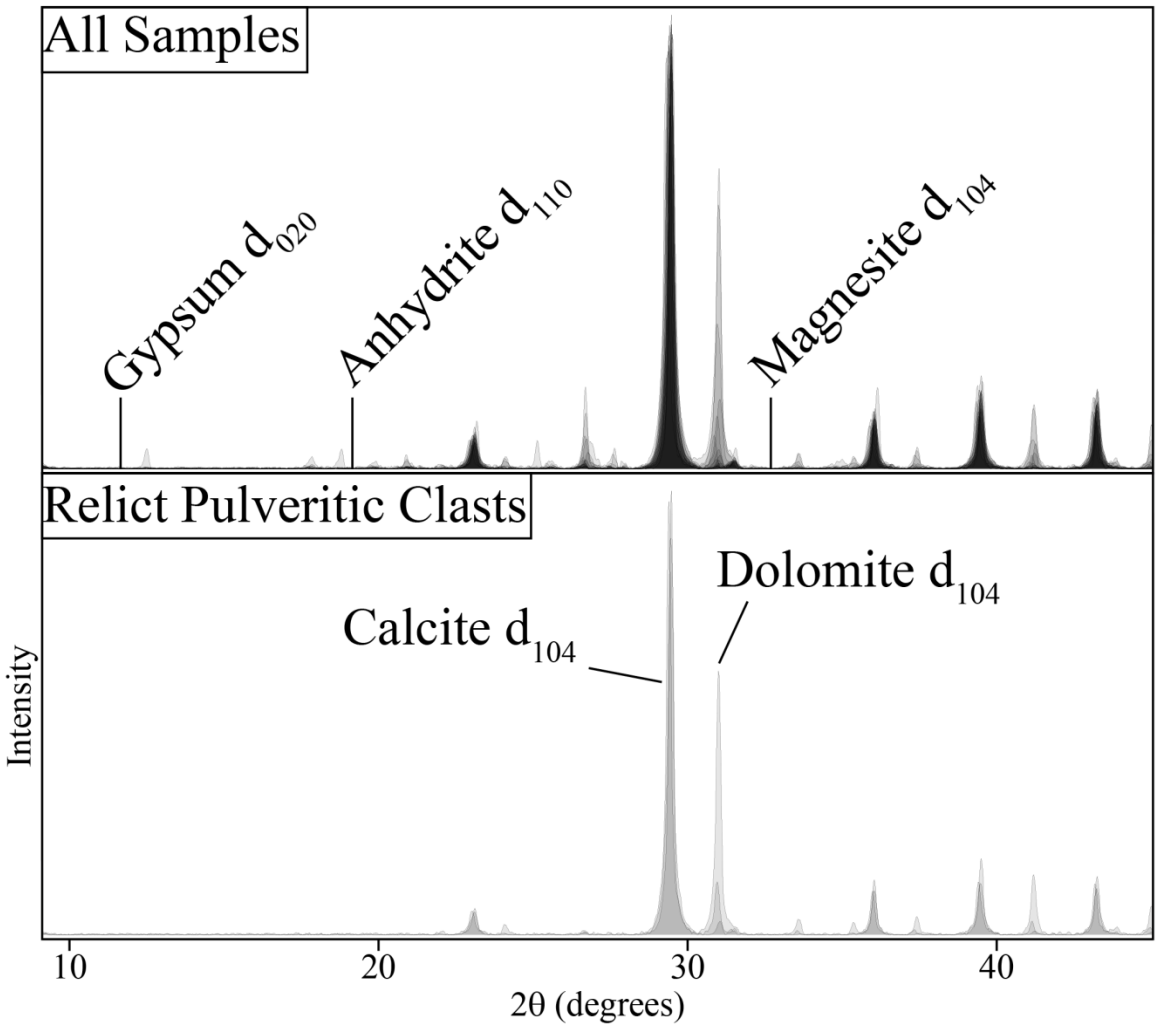

Figure 2.13. XRD spectra of matrix material from seventeen clasts (above), and three samples of relict clast material (below), and the locations of the highest intensity peak of calcite, dolomite, and magnesite carbonate phases, and gypsum and anhydrite sulfate phases. The unlabeled relatively low intensity peaks are a combination of calcite and dolomite peaks, as well as ancillary phases such as quartz and albite. Calcite and dolomite constitute the primary phase in the matrix of all samples, while magnesite and the sulfite phases are absent or at levels below detection limit. Dolomite is present in all three of the relict clasts although in relatively low concentration with respect to calcite in one sample.

2.6 Discussion

2.6.1 Interpretation of petrographic observations

Based on our microstructural observations we conclude that the CV is a tectonite compositionally derived from material tectonically abraded from hanging-wall and foot-wall lithologies. Based on clast volume-percent, most samples are categorically considered breccia or cataclasite, and less often, fault gouge (Passchier and Trouw, 2005). Cataclastic flow is evident by the rigid rotation and translation of clast fragments relative to oneanother, and the infilling of interstitial space between the translational separation of these fragments by fine grained matrix material. Distinctly tectonic fabrics are present in fault gouge samples, and include pressure solution cleavage, pressure shadows, and abraded lenticular clasts.

Compositionally the CV is limited to clast types derived from lithologies in direct contact with the tectonic boundary; however, hanging-wall carbonates tend to compose the majority of clastic material. Evidence of fluid related brittle fracturing is unevenly distributed between upper- and lower-plate rocks. Pervasive dilatational hydraulic fracturing and jigsaw-puzzle brecciation in previously un-deformed rock was observed to be significantly more prevalent in hanging-wall carbonates than in the metamorphic foot-wall. We propose that disaggregation by hydraulic fracturing at the base of the Tuscan nappe facilitated incorporation of hanging-wall material into the cataclastic CV. In contrast, disaggregation of intact foot-wall is limited to mechanical abrasion along the shear-zone interface, and therefore, foot-wall rock is much less likely to be incorporated as cataclastic material.

Our observations support the model of in-situ tectonic development of the CV; however, heterogeneity observed even within our own sample set is evidence of a plurality of distinct processes or local controls responsible for the development of the CV texture. The notion of

local karst reworking of earlier fabric in particular is undeniable due to the prevalence of soluble calcite within the CV, and the presence of several relatively large cave systems situated within along the Alpi Apuane detachment (e.g. Grotto Del Vento). None-the-less, our observations of preserved micro-scale tectonic features preclude whole-sale karstic reworking of the CV. Moreover, the 0.7 mm/yr local uplift rate since 5 Ma (Fellin et al., 2007) leaves little time since the CV was situated below sea-level for thorough karstic re-working at or above the water table.

The complete absence of gypsum and anhydrite in XRD suggests that dissolution of these minerals at depth, a key aspect of the karst model of Alberto et al., (2007), did not play a significant role in the textural development of the CV. Unless dissolution was driven by extensional tectonics, it is unlikely to have been thorough enough as to leave little trace of evaporite minerals, which are abundant elsewhere along tectonostratigraphic base of the Tuscan nappe (e.g. Burano evaporites). The absence of sulfate inclusions in the multiple generations of syn- and post-tectonic veins in the CV, however, suggests that sulfates were not present in great portion as dissolved components during faulting. We therefore argue that if evaporites were present in great abundance, dissolution pre-dated normal faulting, but was not uniquely responsible for the observed CV texture.

A sedimentary origin of the CV fails to account for clast composition, and many of the textures we observed petrographically. Missing are distinctive ophiolite lithologies from the oldest and structurally highest Ligurian nappe. If the CV was deposited as a sedimentary breccia, Liguran ophiolite detritus would necessarily accompany material derived from the structurally lower units. Furthermore, diagenetic crystallization and in-filling of interstitial pore space during lithification of clastic carbonate sedimentary rocks generally serves to increase grain size, and leaves a distinctive pattern of ghost grains in CL; this diagenetic texture is notably absent in the

CV except around very small (<50 μm) matrix grains. Instead, numerous examples of comminution textures, such as jigsaw-puzzle fragmentation are evidence of in-situ tectonic grain-size reduction.

We propose that sedimentary fabrics observed by previous authors are variously related to local fluvial processes within caves, or contained within sedimentary rocks erroneously correlated to the CV. The presence of fossilized Orbulina Unversa foraminifera, which has persisted as evidence of a sedimentary origin of the CV, is only observed in one location (Metato breccia). It is unlikely that delicate fossil features would survive the cataclasis and grain size reduction we observed petrolographically, and therefore, cannot represent deposition prior to emplacement of the Tuscan nappe. Kligfield and Carmignani, (1990) postulated that these fossils instead reside in a younger sedimentary breccia tectonically emplaced within the CV by late stage normal faulting. This younger-breccia hypothesis is supported by the modern existence of Orbulina Universa, which therefore does not require a Miocene depositional age. Indeed some maps of the Apuane region depict this breccia as Quaternary cover, and therefore distinct from the CV (Carmignani et al., 2000). Sedimentary fabrics elsewhere correlated to the CV may be the result of clastic deposition in caves. Subterranean fluvial and lacustrine processes are common within cave environments connected to surface waters and produce clastic sedimentary rocks and associated sedimentary fabrics resembling observed in typical terrestrial deposits (see Bosch and White, 2004). As previously mentioned, extensive cave systems are present in the Alpi Apuane region; distinctly sedimentary fabrics described by proponents of a sedimentary origin of the CV may be exhumed clastic sedimentary rocks originally deposited in one of these cave systems.

2.6.2 Stratigraphic relationship

The CV is commonly equated to a Triassic evaporates found elsewhere stratigraphically at the base of the Tuscan Nappe (e.g. Merla, 1951; Baldacci et al., 1967; Carmignani and Kligfield, 1990; Costagliola et al., 1999; Lugli, 2001; Lugli et al., 2002, and others). This correlation is useful for a variety of textural and compositional comparisons with examples of this Triassic succession found elsewhere in the Apennines. We argue that the CV is not a stratigraphic unit, but instead a fault rock that shares a tectonic, rather than stratigraphic, position with evaporates found at the base of the Tuscan nappe. The CV is considered a stratigraphic unit composted of a polygenic breccia of either Ladinian-Norian (Decandia et al., 1968), or Norian-Rhaetian age (Carmignani et al., 2000), and is commonly correlated with the tectonized evaporite rich Burano formation in the Secchia valley, NE of the Alpi Apuane core. The Burano fm. in the Secchia river valley is similarly considered an upper Triassic unit, and comprises hydrothermally and tectonically altered evaporates and carbonates. While general stratigraphy is difficult to determine in the Burano fm., its sedimentary character and composition is preserved to a degree sufficient to make first order inferences regarding its depositional environment. Some authors use Calcare Cavernoso as a textural term sensu-strictu, and regard the CV of the Apuane region as belonging to the Burano fm. (e.g. Lugli, 2001; Lugli et al., 2002). However, aside from its position at the base of the Tuscan nappe, the CV shares few similarities with the Burano formation. In the CV, evaporate minerals (i.e. gypsum, anhydrite), and magnesite, common in the Burano fm., are not observed in the field and are below detectable levels in our samples. Instead, the CV is compositionally derived from tectonically incorporated clasts of a variety of sedimentary and meta-sedimentary units. The age of the CV tectonic breccia should not be considered older than its constituent parts, which is limited to Miocene and younger by the metamorphic age of the Alpi Apuane metamorphic core.

Rather than a stratigraphic equivalency between the CV and Burano fm., we suggest a common relationship with a tectonic boundary. The Burano fm. served as the thrust decollement upon which the Tuscan nappe was emplaced during accretion. The CV was formed along this same structure during its reactivation as an extensional detachment exhuming the Alpi Apuane core, as discussed below. Both units therefore occupy a common tectonic horizon, rather than the necessarily Triassic base of the Tuscan nappe stratigraphic succession.

2.6.3 T-P-t of faulting

Contrasting exhumation models predict starkly different P-T conditions during slip along the Alpi Apuane detachment. Carmignani and Kligfield (1990)'s exhumation model attributes uplift and cooling of the metamorphic core to pervasive extensional attenuation and normal-slip along the Alpi Apuane detachment at mid-crustal levels. Mid-crustal slip along the Alpi Apuane detachment is supported by estimated fault-zone fluid trapping conditions at 300-345 ^{o}C based on fluid inclusions (Hodgkins and Stewart, 1994). Assuming a geothermal gradient of ~31 ^{o}C/km, Hodgkins and Stewart (1994) concluded that the fault was last active at 10 km depth. Conversely, some authors interpret extension in Northern Apennines as driven by mid-crustal thickening (Carmignani et al., 1978; Boccaletti et al., 1983; Cello and Mazzoli, 1996; Jolivet et al., 1998). Kilometer-scale ductile structures, that form the basis of Carmigani and Kligfield (1990)'s model, have alternatively been interpreted as evidence shortening, rather than extension (Boccaletti et al., 1983; Carosi et al., 2002, 2004). The structural position of the relatively higher grade Massa unit above the Apuane unit demands at least some amount of mid-crustal stacking contemporaneous with exhumation of the metamorphic core. In this latter interpretation, exhumation of the metamorphic core from peak P-T conditions to upper-crustal conditions is attributed to under-plating rather than slip along the Alpi Apuane detachment, and is complete by

10-13 Ma, as evidenced by similar zircon fission track ages in both the Apuane and Massa units (Fellin et al., 2007).

The on-set of upper-crustal extension in this portion of the Northern Apennines is marked by the late Miocene deposition in the Via Reggio basin which began ~7 Ma (Bernini et al., 1990). Early extension is contemporaneous with cooling of the Alpi Apuane metamorphic core to upper-crustal conditions, and the on-set of exhumation of the Tuscan nappe is evidenced by cooling to below the closure temperature of zircon U-Th/He at 13-14 Ma. Beginning 10-13 Ma, the metamorphic foot-wall and anchizonal hanging-wall cooled together, except for a brief period of differential cooling between 6-4 Ma. Differential cooling accounts for approximately 3-4 km of missing vertical section between the closure temperatures of zircon and apatite U-Th/He, which Fellin et al. (2007) attribute to slip along the Alpi Apuane detachment. Brittle fabrics within the CV support the interpretation that the Alpi Apuane detachment was active at very shallow crustal levels. The fine grained pulveritic matrix in the CV breccia and cataclasite shows no signs of dynamic recrystallization or annealing, which are observed in foot-wall marbles and typify carbonates deformed in the temperature range estimated by Hodgkins and Stewart (1994) (300-350^{o}C). The common presence of saddle dolomite reflects fluid temperatures between 60-150 ^{o}C (Radke and Mathis, 1980), consistent with the 60-170 ^{o}C range between the closure temperatures of zircon and apatite U-Th/He.

Fellin et al. (2007) suggest that higher temperature (300-340^{o}C) estimates of fault slip as related to local hydrothermal activity. However, these results were relatively consistent between 25 samples distributed along approximately 40 km of the Alpi Apuane detachment, which is difficult to attribute to a local process. It is possible that the sampling strategy of Hodgkins and Stewart (1994) preferred fabrics produced in an earlier stage of detachment slip at greater depths.

The majority of fault zone samples from Hodgkins and Stewart (1994) were collected from quartz veins; in our samples quartz veins were restricted to foot-wall clasts or re-worked fragments, but were not included in the latest stage brittle deformation fabrics. Alternatively, a relatively low assumed crustal density of 2.45 g/cm^3 in Hodgkins and Stewart (1994)'s pressure correction may have exaggerated temperature estimates. Moreover, these authors base their tectonic conclusions on maximum pressure and temperature measurements, which correlate well with the interpretation of mid-crustal detachment slip of Carmignani and Kligfield (1990). We observe progressive re-working of the CV breccia, therefore, estimates of latest-stage faulting are more appropriately recorded in minimum rather than maximum P-T conditions. Assuming an upper-crustal density of 2.7 g/cm^3 these estimates could be as low as 240 ^{o}C at 7.4 km depth, in agreement with the geothermal gradient calculated by Fellin et al (2007), and our own observations of type II calcite twinning, which typically forms between 200-300 ^{o}C (Groshong et. al., 1984; Rowe and Rutter, 1990; Ferrill, 1991; Ferrill et al., 2004). Temperatures above 240 ^{o}C exceed the thermal maximum of the Tuscan nappe estimated by un-reset zircon fission track ages (Fellin et al., 2007). However, this thermal maximum was measured in the Macigno, the stratigraphically upper-most portion of the Tuscan nappe and some 2-3 km above its base. Ambient temperatures in the CV may therefore have reached as high as ~300 ^{o}C during early stages of uplift and exhumation.

2.7 Conclusions

We emphasize three main points: first, the CV is a tectonite with preserved micro-scale tectonic fabrics; second, brittle fabrics preserved within the CV indicate that slip along the Alpi Apuane detachment occurred at shallow crustal levels; third, the CV should not be considered a stratigraphic unit with a Triassic depositional age.

Ambiguity regarding the genetic origin of the CV is likely due to an absence of primary data in the published literature, and interpretive differences of observed fabrics. Proponents of a tectonic origin of the CV describe brittle tectonic fabric (e.g. Carmignani and Kligfield, 1990); authors in favor of a sedimentary origin have declared absence of tectonic fabric everywhere and instead point to the presence of laminar stratification and cross bedding (e.g. Federici and Raggi, 1974); still others provide hybrid interpretations, such as the presence of tectonic fabric in along the eastern margin but an absence of such fabric along the western margin of the metamorphic core (e.g. Feroni et al., 1976). Rarely, however, are data associated with these described observations presented in the literature or on published maps of the Alpi Apuane. The presence of foot-wall clasts affirms, on a compositional basis, a tectonic origin of the CV due to the thermochronometrically determined timing of metamorphism and exhumation of the Alpi Apuane metamorphic core which post-dates emplacement of the Tuscan nappe. Moreover, micro-scale fabrics are typical fault related fabrics, and difficult to produce with depositional processes alone.

Structural interpretation of ductile foot-wall fabrics, and at least one fluid inclusion study suggest that slip along the Alpi Apuane detachment may have occurred at depths of 10 km or greater. These fabrics are not however preserved in the CV, instead, evidence of cataclastic flow and hydraulic fracturing is indicative of tectonization at shallow crustal conditions, and consistent with differential cooling between the hanging-wall and foot-wall between the closure temperatures of zircon and apatite U-Th/He (170-60 ^{o}C). Slip along the Alpi Apuane detachment at deeper crustal levels associated with early uplift of the metamorphic core is unlikely to be recorded in the CV, which is predominantly composed of Tuscan nappe carbonate clasts, which never exceeded 240 ^{o}C. Whether or not normal slip along the Alpi Apuane detachment

penetrated into the middle crust, the brittle nature of the CV indicates that extension along low-angle normal faults was active in the upper-crust.

The CV is composed primarily of limestone clasts, cataclastic matrix, and Miocene aged metasedimentary clasts combined as a clastic tectonite during Mio-Pliocene detachment slip, and does not constitute a stratigraphic unit. While the CV shares the stratigraphic base of the Tuscan nappe with geographically wide-spread evaporites (e.g. Burano fm.), any correlation between these two units is not supported by composition or a shared genetic history. Instead, the CV and Burano fm. are more appropriately linked by a shared tectonic relationship. These relatively weak basal evaporites were utilized as a thrust decollement during emplacement of the Tuscan nappe. Subsequently, the CV was formed along this slip-plane during reactivation as a detachment.

Chapter 3: Kinematics of Neogene slip along the Saddle Mountains thrust

3.1 Introduction

Active-source seismic reflection profiles provide direct insight into subsurface structural features, and are particularly valuable where surface exposure is limited. The goal of this paper is to make available, for the first time, a seismic reflection profile clearly depicting the geometry of subsurface folds beneath the Saddle Mountains anticline (SMA) in eastern Washington, and to provide kinematically viable structural interpretations of sub-surface structures discernible within this dataset. Our aim is to address some aspects of the long standing debate surrounding the nature of faulting in the Yakima fold and thrust belt (YFTB) – thin-skinned vs. thick-skinned tectonics, a debate which has significant implications for assessment of regional seismic hazards.

3.2 Geologic background

The Yakima fold and thrust best in eastern Washington is composed of a series of low relief (typically <600m) E-W to NW-SE trending asymmetric anticlinal ridges arranged in a roughly en echelon arrangement and separated by broad (~20 km) low-amplitude synclinal valleys (Watters, 1989) (Fig. 3.1). Anticlinal ridges are interpreted as fault-related hanging-wall folds and are typically bound along their relatively steep north flanks by north verging thrust or reverse fault traces (Bentley, 1977; Goff, 1981; Hagood, 1986; Reidel, 1984, 1989). Faulting and folding in the YFTB deforms middle to late Miocene CRBG (17-6 Ma) (Reidel et al., 1984, 1989) and late Miocene and younger fluvial deposits, which in some places can be found at the crests of anticlinal ridges. Where hydrocarbon exploration boreholes have penetrated the CRBG the underlying strata are composed of Tertiary non-marine sedimentary rocks (Campbell, 1989),

although the depth to which the folding and faulting observed in the surface geology penetrates has not been definitively resolved.

The onset of shortening in the YFTB is unknown; however, thinning of the Grand Ronde Basalt Formation (16.5-15.6 Ma) of the CRBG in the SMA requires a topographic high coincident with the crest of the anticline by middle Miocene (Reidel, 1984; Reidel, et al., 1989). Subsequent sustained uplift in the SMA is recorded by the progressive on-lapping of middle to late Miocene Wanapum and Saddle Mountains Basalt Formations (15.6 - 6 Ma) (Reidel, 1984). Post CRBG shortening resulted in uplift of the upper Miocene-lower Pliocene Ringold Formation, fluvial deposits that cap the CRBG basalts, and the present structurally controlled relief (Reidel et al., 1989).

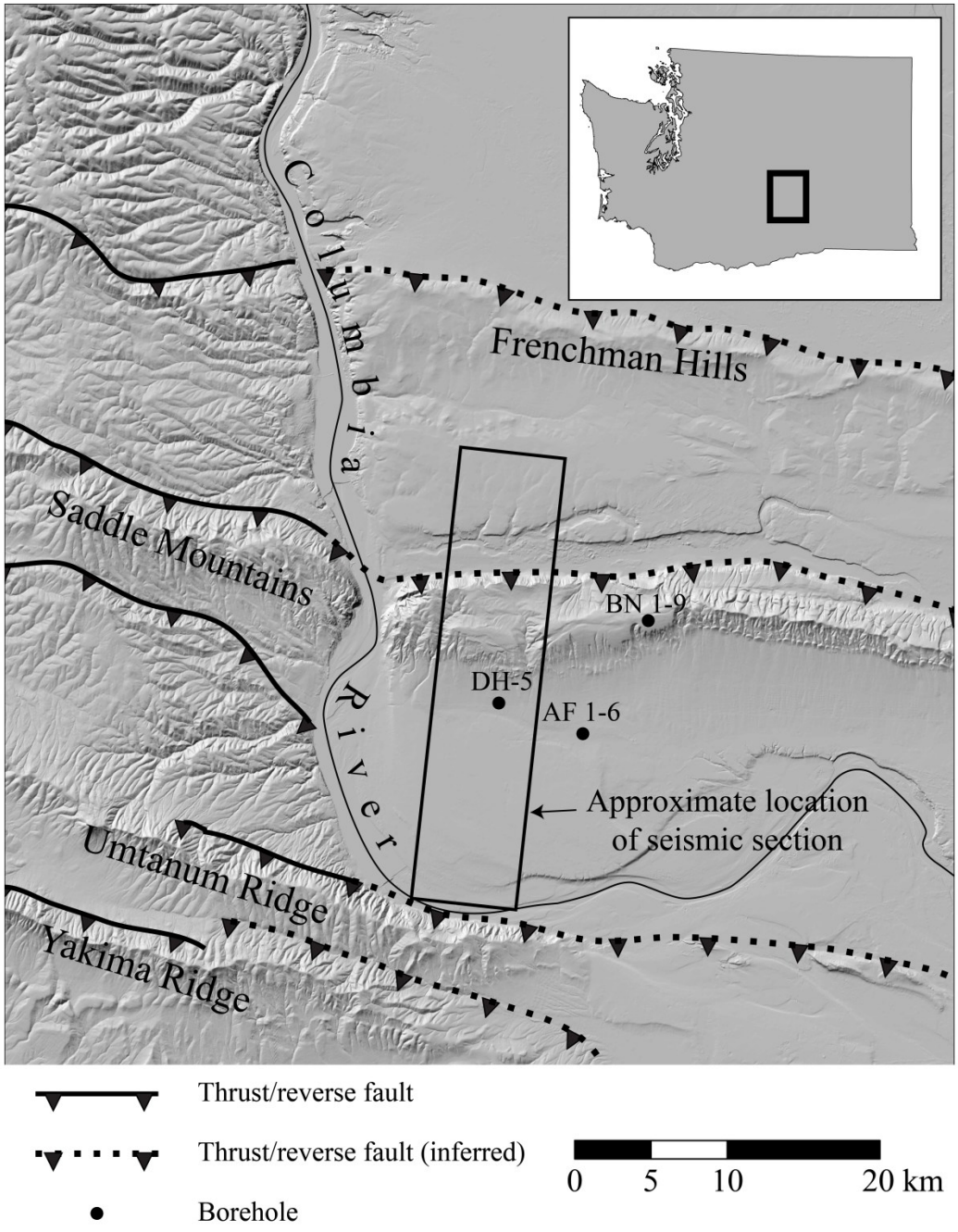

Figure 3.1. Shaded relief map of the Yakima fold and thrust belt in the vicinity of the Saddle mountains anticline. Major thrust structures and anticlinal ridges from Reidel and Fetch (1994). Approximate location of the seismic section as indicated by the rectangle.

Geologic and geodetic observations indicate that shortening across the YFTB is ongoing. Trenching along the Saddle Mountains fault at Smyrna Bench (West et al., 1996), and at Hessler flats on the southern flank of the Umtanum ridge (Blakely et al., 2011) have yielded offsets in late-Quaternary colluvial deposits. Geodetic measurements record active shortening across the Columbia plateau (McCaffrey et al., 2000, 2007; Mazzotti et al, 2002). McCaffrey et al., (2007) report a .424o Ma-1 difference in angular velocity between the YFTB block and the Wenatchee block about a common Euler pole located 400 km to the SE of the SMA in Idaho, which translates into a convergence rate of approximately 2.7 mm/yr regionally. A portion of this modern shortening is likely localized along the Yakima thrust faults and presents the primary seismic hazard to the Hanford nuclear site and several major dams situated along the Columbia river. Predicted maximum magnitude seismic events range from 5.2-7.8 moment magnitude for the structures in the YFTB (PSHA); however, these predictions are based on empirical relationships (Wells and Coppersmith, 1994), including fault geometry, which are not well known.

How shortening is accommodated and the first order geometry of the Yakima thrust structures remain a topic of debate. At the core of this debate is disagreement regarding two fundamental structural characteristics that determine hazard potential of active structures: dip angle, and depth of faulting (see Wells and Coppersmith, 1994). Does slip along exposed surface faults sole into decollement horizons at depth, or occur along reverse faults that penetrate and offset crystalline basement?

The general absence of independent estimates of total shortening, and limited fault surface exposure and borehole data give little insight into the subsurface fault geometry. Interpretations of fault dip are widely variable and are derived from a variety of often circumstantial

observations, such as along strike projection of distant features (e.g. Beeson and Moran, 1979; Tolan and Beeson, 1984; Tabor et al., 1984; Cheney and Hayman, 2009) or are subject to a range of assumptions which are difficult to determine, such as gravity inversion of subsurface bodies with unknown densities and possible non-tectonic basement topography (e.g. Catchings and Mooney, 1988; Saltus, 1993; Blakely et al., 2011; see discussion in Catchings and Saltus, 1994).

3.3 Methods

Fault geometry has a systematic influence on specific aspects of superjacent folds (Rowan and Linares, 2000; Allmendinger and Shaw, 2000; Wilkerson et al., 2002) and kinematic models have long been utilized to study fault-related folding (e.g. Suppe, 1983; Wilkerson et al., 1991; Salvini and Storti, 2001). Flexural slip-based kinematic models (e.g. Suppe, 1983) are useful for inferring fault geometry in stratified rocks where estimates fold geometry are available (Savage and Cooke, 2003). We determined stratigraphic and geometric fold relationships within the SMA with a previously unpublished seismic reflection profile, borehole logs (Shell Oil Co., BN 1-9; Sierra Geophysics and Rockwell Hanford Operations, DH-5; Delta Petroleum Corp., Andersonville Farms 1-6) (Fig. 3.2), and published surface geologic data (Reidel, 1988; Reidel and Fecht, 1994). With these geometric and stratigraphic data we determined plausible end member fault geometries and slip values capable of producing the folding observed within the SMA via balanced kinematically restorable cross-sections constructed using iterative forward modeling techniques in Midland Valley's 2D Move structural modeling software.

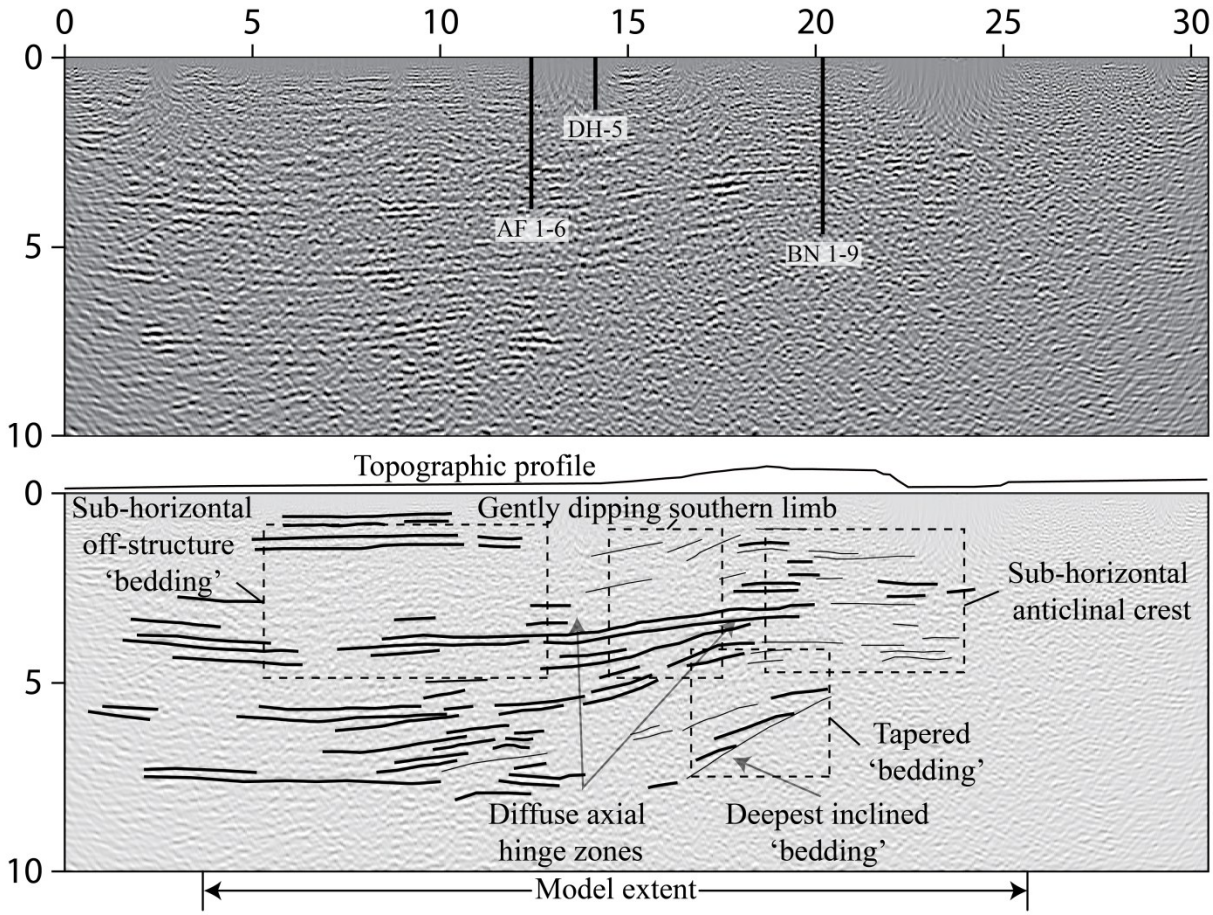

Figure 3.2. Seismic reflection profile with approximate locations of projected boreholes (top) and ornamented seismic reflection profile with topographic trace and horizontal extent of our kinematic models (bottom). Line thickness indicates relative interpretation confidence, discernible geometric relationships are labeled and outlined by dashed boxes and described in the text.

Direct identification of fault horizons was hindered by relatively poorly resolved reflectors. Instead we relied on discernible geometric relationships of planar features at depth, which we have highlighted in figure 3.2. South of the topographic expression of the SMA, prominent reflectors are sub-horizontal to some 6-7 km depth. Beneath the southern limb of the SMA gently south-dipping reflectors (~7^{o}) are consistent with surface basalt flow-top attitude measurements. From the crest of the anticline towards the north, shallow reflectors (< 4 km depth) are again horizontal. No discrete axial hinge separates the regions of horizontal and inclined reflectors; instead, this change in orientation occurs gradually over several kilometers in diffuse axial hinge zones. In contrast to shallow sub-horizontal reflectors, between 5-8 km reflectors directly beneath the crest of the SMA dip relatively steeply towards the south, and no horizontal reflectors are apparent within the lateral topographic confines of the SMA. The transition from steeply dipping reflectors at depth to horizontal beds in the shallower portion of the section appears to occur gradually with dip angles ranging from ~20o at 8 km in the deepest inclined reflectors, to ~12o at 5 km. We interpret this portion of the section as tapered bedding either related to syn-tectonic onlapping, or syn-tectonic erosion and deposition. Boreholes BN1-9 and Andersonville Farms 1-6 both penetrate the entire thickness of the CRBG at a depth roughly coincident with two prominent reflectors located at approximately the transition between deep inclined reflectors and shallow horizontal reflectors in the core of the SMA. However, these wells are located some 5-7 km off section and exact correlation with the sub-surface seismic stratigraphy is hindered by lateral variation in accumulated strain, non-coaxial strain, and local thickness variations of the CRBG flows along the SMA.

Fault geometry determined by the inversion of overlying fault related folding is dependent upon the on slip method. We modeled the SMA using the fault bend folding algorithm in 2D Move

which is commonly applied to fault-related folds in fold-and-thrust belts, and preserves bed length and 2D cross sectional area (Suppe, 1983). Fault-bend folding assumes hanging-wall distortion by flexural slip along flow contacts and is consistent with field observations of bedding-parallel slip scarps in the CRBG at several locations within the Yakima folds (e.g. Price and Watkins, 1989; Blakely et al., 2011). It is difficult to evaluate the applicability of the fault-bend fold slip method beneath the CRBG; however, preserved bedding apparent in the seismic section argues against alternative models such as flexural flow, or detachment folding (e.g. Watters, 1989) which would disrupt bedding.

3.4 Results

Low-angle near-surface faulting beneath the SMA accompanied by a decollement horizon following the base of the CRBG adequately reproduces the surface structural pattern with 350-450 m of heave (Fig. 3.3). However, this low angle fault cannot readily account for inclined bedding observed at depth. Deformation below the CRBG requires an additional detachment soling into a decollement located at approximately 8-9 km. Syn-convergence deposition of pre-CRBG sediments is necessary in order to account for tapered bedding along the lower decollement with decreasing total heave reflected in up-section folds. Along the lower decollement, the deepest beds require a minimum 7.6km of heave. Of this 7.6 km, approximately 3.2 km occurs after deposition of the CRBG as is evident by folding of the prominent base-CRBG reflector; although, it is possible that apparent folding of the basal contact is in part related to on-lapping of the CRBG upon pre-existing structurally controlled topography, as is observed higher in the section (See Reidel, 1984). This relationship, however, does not affect our heave estimates, which are necessary to account for present topography.

Both near surface and deeper folding beneath the SMA can alternatively be accounted for by slip along a single listric reverse fault soling into a decollement at approximately 8-9 km. Similar to the two decollement model, tapered bedding at depth below the SMA crest is accounted for by on-lapping of syn-convergence pre-CRBG sediments. Inclination of the most deeply and steeply dipping beds requires a minimum 2 km of decollement heave, of which ~600 m occurs after emplacement of the CRBG. The listric bending of the high-angle fault model is necessary to account for the relatively gentle dip of the south-dipping anticlinal back limb observed in both the surface geology and at depth, as discussed below.

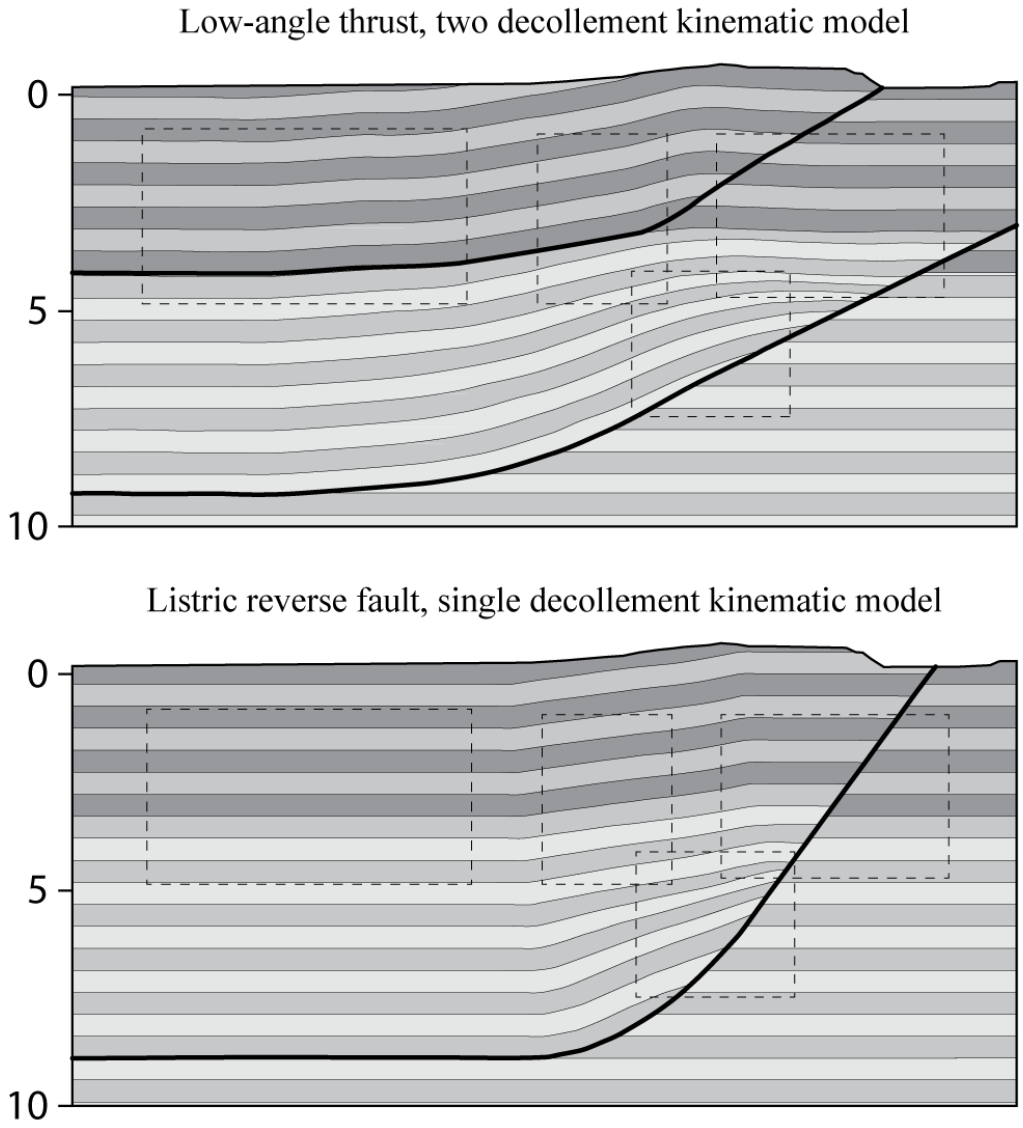

Figure 3.3. Representative kinematically viable end member models based on the fault-bend-fold algorithm (bed-parallel flexural slip, see Suppe, 1983) in Midland Valley Move structural modeling software. Dashed boxes correspond to the dashed boxes in Fig. 3.2. Alternating light gray bands correspond to sub-CRBG rocks, perhaps including crystalline basement in the deepest portion of the section, alternating dark gray bands indicate CRBG. Both the two fault model (above) and single fault model (below) account for greater folding in the deeper portion of the SMA with a combination of syn-tectonic deposition, and progressive shortening. In the two fault model (above), the difference in fold amplitudes between deep and shallow structures are accomplished in part by different total slip along the two decollement horizons. The upper decollement is broadly folded by slip along the lower decollement, thus both structures must have been active concurrently. In the single fault model (below) this amplitude difference in shallow and deep fold amplitudes is accomplished by syn-tectonic deposition alone.

3.5 Discussion

Since no independent data are available to identify which, if any, of the reflectors in the seismic section represent the fault plane or planes, our kinematic models are aimed at satisfying the discreet relationships presented in Fig. 3.2. Subsurface folding in the SMA that is kinematically reproduced by hanging-wall deformation above a low angle thrust fault or alternatively above a high angle reverse fault requires specific geometric attributes. These geometric attributes bear directly upon previous interpretations of the timing and kinematics of fault related folding in the YFTB.

3.5.1 Timing of anticlinal growth

The onset of shortening in the YFTB is unknown, but is considered to post-date the deposition of Eocene sub-CRBG sedimentary rocks. These sub-CRBG rocks are interpreted as syn-extension sediments deposited in fault-bounded grabens (Cashman and Whetten, 1976; Tabor et al., 1982, 1987; Johnson, 1985; Taylor et al., 1988; Evans, 1994; Catchings and Mooney, 1988). As an alternative, Cheney and Hayman (2009) proposed that these 'grabens' are synclinal basins between reverse faults; thus deposition accompanied shortening rather than extension. Tapered bedding of the sub-CRBG clastics, apparent in the seismic section deeper than ~4 km and beneath the crest of the SMA (Fig. 3.2), is evidence of on-lapping upon growing anticlinal structures; this on-lapping pattern supports the latter hypothesis that deposition accompanied shortening and uplift, implying active shortening in the YFTB since at least late Eocene time.

3.5.2 Decollement slip and basement uplift

At the core of the thin-skinned vs. thick-skinned tectonics debate in the YFTB is the question of whether or not basement rocks are involved in the faulting observed in the surface geology or alternatively slip is localized upon decollement horizons. It is important to clarify that in this

paper we distinguish crystalline metamorphic or igneous rocks as basement and Paleocene-Oligocene clastics as sub-CRBG sedimentary rocks.

Previous authors have employed a range of methods aimed at elucidating specific geometric criteria to either support or preclude a link between observed surface deformation in the YFTB with faulting at depth. Several important observations have fueled the debate regarding this link. First, major (10s of km scale) basement structures have been observed in outcrop along the margins of the CRBG (Miller and Bowring, 1990; Patterson et al., 2004; Cheney and Hayman, 2009) and beneath the YFTB in gravity (Blakely et al., 2011), seismic reflection (Jarchow et al., 1994), and seismic refraction (Catchings and Moony, 1988) investigations. The nature of this basement topography is unknown and is alternatively attributed to reverse faulting spatially linked to surface faults (Blakely et al., 2011), or normal faulting that predates modern shortening (Catchings and Moony, 1988). Second, several authors have noted structural differences in the orientation of structural trends and a lateral offset of hinge lines (Campbell, 1989), and a distinct contrast in finite strain between folding in the sub-CRBG clastic rocks and the CRBG (Campbell, 1989; Cheney and Hayman, 2009). Greater finite strain within the sub-CRBG folds observed in outcrop along the NW margin of the CRBG is consistent with our interpretation that folding began prior to emplacement of the CRBG. Campbell (1989) suggests that lateral offset and variation in the orientation between the Yakima folds and underlying structures is perhaps the result of distributed slip along small structures, or offset along an intervening decollement horizon. However, Reidel (1989) argues that little decollement slip is required to produce the relatively long wavelength low amplitude folds.

While our two kinematic models solve for folding differently, both models require decollement slip at depth. Nowhere in the seismic section does the back-limb of the SMA exceed ~20-30o,

and with a few local exceptions field and borehole measurements are typically 10o or less. In the high-angle fault model this inclined back-limb is not steep enough to account for slip along a simple high-angle fault. Suppe (1983) demonstrated that multi-bend faults produce hanging-wall anticlinal back-limbs inclined at an angle equal to the sum of the change of the fault dip beneath the hanging-wall over the slip heave (i.e. fault curvature, see Suppe, 1983 eq. 18 & 21). The principle that the inclination of the back-limb of the hanging-wall fold is related to fault curvature rather than fault dip implies that even very high-angle fault can produce gently inclined back-limbs in hanging-wall folds (e.g. Erslev, 1986), provided that total heave does not exceed the horizontal length of the curved and inclined ramp (Fig. 3.4a). In the high angle fault model the inclination of the back-limb of the SMA must therefore reflect the curvature of a listric fault geometry.

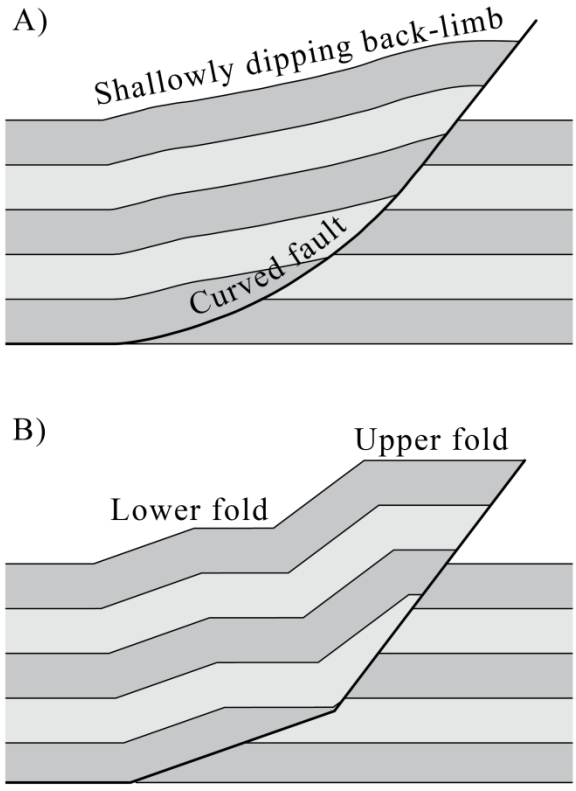

Figure 3.4. (A) Hanging-wall back-limb inclination is determined by the curvature of the underlying fault; this principal implies that high-angle faults can produce shallowly inclined back-limbs. (B) Fault kings, or changes in fault curvature are reflected in a change in inclination of the back-limb of the hanging-wall fold. Thus a single kinked fold may effectively produce a pair of laterally offset folds with varying amplitudes.

Our high-angle listric fault model is at odds with the interpretation that the Yakima faults originate in the middle crust: we note the general absence of mechanical stratigraphy in crystalline basement conducive to decollement slip. Arguably some degree of shallowing of the anticlinal back-limb could be accomplished by on-lapping of syn-tectonic sediments rather than fault bending as we propose. However, the preservation of shallowly inclined beds at depth, and no clear kinking of deeply buried beds, as would be expected with progressive slip, suggests that surface processes are not responsible for the observed geometry.

Lateral offset and finite-strain variation between folds within and below the CRBG is readily accounted for in our two-decollement model by differences in fault geometry and total slip between the two faults. A similar geometric relationship is achieved with a single fault by a lateral variation in curvature, which will result in multiple and apparently distinct hanging-wall folds. This relationship is demonstrated schematically in Fig. 3.4b, where two distinct hanging-wall folds are produced as a result of two discrete fault bends. In this simplified model the wavelength and amplitude are controlled by cut-off angle and total slip. It is important to note that since in this model the fault dip decreases with depth, the upper fold will have a shorter wavelength and higher amplitude. In our seismic section, and in observations of sub-CRBG folding along the NW margin of the CRBG, deeper folds have greater amplitudes. In both of our kinematic models of the SMA, greater amplitude folds at depth are accounted for by slip prior to emplacement of the CRBG, as previously discussed.

3.6 Conclusions

We present a previously unpublished seismic section and provide categorically representative end-member kinematic models of high- and low-angle faults that satisfy the geometric relationships within CRBG and underlying sedimentary strata beneath the SMA. The relatively poor quality seismic data do not allow us to directly determine the geometry of the fault or faults beneath the SMA. However, principles of kinematic forward modeling of hanging-wall folds with fault-bend-fold geometry allow us to elucidate several important relationships central to our understanding of how shortening is accommodated in the YFTB. We emphasize three main points: (1) shortening within the YFTB was active during deposition of the sub-CRBG Eocene-Oligocene clastics. (2) Regardless of initial fault geometry, soling of the Yakima faults into decollement horizons is necessary to satisfy kinematic constraints. (3) Lateral offset and

differences in strain accumulation between deep and shallow folds are readily explained by, but do not necessitate, structural independence.

Since many important features necessary to fully describe the sub-surface structural pattern beneath the SMA are sub-seismic, the models presented here should be considered representative. Latitude in interpretations is illustrated by the significant geometric contrasts between our two models. Nonetheless, our models adhere to the available geometric constraints, and our heave estimates are consistent with previous estimates along the SMA fault. We suggest that these values are useful as order of magnitude estimates but inappropriate for quantitative assessment of short-term slip rates.

References cited

Abbate, E., and Bruni, P., 1987, Torbiditi Oligo-Mioceniche ed evoluzione del margine Nord-Appenninico: Mem. Soc. Geol. Ital., v. 39, p. 19-33.

Alberto, W., Carraro, F., Giardino, M., and Tiranti, D., 2007, Genesis and evolution of 'pseudocarniole': preliminary observations from the Susa Valley (Western Alps): Geological Society, London, Special Publications, v. 285, p. 155-168.

Allmendinger, R.W., and Shaw, J.H., 2000, Estimation of fault propagation distance from fold shape: Implications for earthquake hazard assessment: Geology, v. 28, p. 1099.

Baldacci, F., Elter, P., Giannini, E., Giglia, G., Lazzarotto, A., Nardi, R., and Tongiorgi, M., 1967, Nuove osservazioni sul problema della falda toscana e sulla interpretazione dei flysch arenacei tipo "Macigno" dell'Appennino Settentrionale: Mem. Soc. Geol. It, v. 6, p. 213-244.

Balestrieri, M., Pandeli, E., Bigazzi, G., Carosi, R., and Montomoli, C., 2011, Age and temperature constraints on metamorphism and exhumation of the syn-orogenic metamorphic complexes of Northern Apennines, Italy: Tectonophysics.

Balestrieri, M.L., Bernet, M., Brandon, M.T., Picotti, V., Reiners, P., and Zattin, M., 2003, Pliocene and Pleistocene exhumation and uplift of two key areas of the Northern Apennines, Pergamon-Elsevier Science Ltd, p. 67-73.

Beeson, M.H., and Moran, M.R., 1979, Stratigraphy and structure of the Columbia River Basalt Group in the Cascade Range, Oregon, in Hull, D.A., and Riccio, J.F., eds., Geothermal resource assessment of Mt. Hood Oregon Department of Geology and Mineral Industries, p. 5-77.

Bennett, R.A., Hreinsdóttir, S., Buble, G., Basic, T., Bacic, Z., Marjanovic, M., Casale, G., Gendaszek, A., and Cowan, D., 2008, Eocene to present subduction of southern Adria mantle lithosphere beneath the Dinarides: Geology, v. 36, p. 3.

Bentley, R.D., 1977, Stratigraphy of the Yakima basalts and structural evolution of the Yakima ridges in the western Columbia Plateau: Geological Excursions in the Pacific Northwest, p. 339-389.

Bernet, M., Brandon, M., Garver, J., Balestieri, M., Ventura, B., and Zattin, M., 2009, Exhuming the Alps through time: clues from detrital zircon fission-track thermochronology: Basin Research, v. 21, p. 781-798.

Bernini, M., Boccaletti, M., Moratti, G., Papani, G., Sani, F., and Torelli, L., 1990, Episodi compressivi neogenico-quaternari nell'area estensionale tirrenica nord-orientale. Dati in mare ea terra: Mem. Soc. Geol. Ital, v. 45, p. 577-589.

Blakely, R.J., Sherrod, B.L., Weaver, C.S., Wells, R.E., Rohay, A.C., Barnett, E.A., and Knepprath, N.E., 2011, Connecting the Yakima fold and thrust belt to active faults in the Puget Lowland, Washington: Journal of Geophysical Research, v. 116, p. B07105.

Boccaletti, M., Capitani, S., Coli, M., Fornace, G., Gosso, G., Grandini, G., Milano, P., Moratti, G., Nafissi, P., and Sani, F., 1983, Caratteristiche deformative delle Alpi Apuane settentrionali: Mem. Soc. Geol. It, v. 26, p. 527-534.

Boccaletti, M., and Sani, F., 1998, Cover thrust reactivations related to internal basement involvement during Neogene-Quaternary evolution of the northern Apennines: Tectonics, v. 17.

Boggs, S., and Krinsley, D., 2006, Application of cathodoluminescence imaging to study of sedimentary rocks, Cambridge University Press, 163 p.

Bosch, R.F., and White, W.B., 2004, Lithofacies and transport of clastic sediments in karstic aquifers, *in* Sasowsky, I.D., and Mylroie, J., eds., Studies of cave sediments: New York, Kluwer Academic/Plenum, p. 1-22.

Boschetti, T., Venturelli, G., Toscani, L., Barbieri, M., and Mucchino, C., 2005, The Bagni di Lucca thermal waters (Tuscany, Italy): an example of Ca-SO< sub> 4</sub> waters with high Na/Cl and low Ca/SO< sub> 4</sub> ratios: Journal of Hydrology, v. 307, p. 270-293.

Brandon, M.T., Roden-Tice, M.K., and Garver, J.I., 1998, Late Cenozoic exhumation of the Cascadia accretionary wedge in the Olympic Mountains, northwest Washington State: Geological Society of America Bulletin, v. 110, p. 985-1009.

Brichau, S., Ring, U., Carter, A., Bolhar, R., Monie, P., Stockli, D., and Brunel, M., 2008, Timing, slip rate, displacement and cooling history of the Mykonos detachment footwall, Cyclades, Greece, and implications for the opening of the Aegean Sea basin: Journal of the Geological Society, v. 165, p. 263-277.

Brunet, C., Monié, P., Jolivet, L., and Cadet, J.P., 2000, Migration of compression and extension in the Tyrrhenian Sea, insights from 40Ar/39Ar ages on micas along a transect from Corsica to Tuscany: Tectonophysics, v. 321, p. 127-155.

Burchfiel, B.C., Nakov, R., Dumurdzanov, N., Papanikolaou, D., Tzankov, T., Serafimovski, T., King, R.W., Kotzev, V., Todosov, A., and Nurce, B., 2008, Evolution and dynamics of the Cenozoic tectonics of the South Balkan extensional system: Geosphere, v. 4, p. 919-938.

Campbell, N.P., 1989, Structural and stratigraphic interpretation of rocks under the Yakima fold belt, Columbia Basin, based on recent surface mapping and well data: Volcanism and Tectonism in the Columbia River Flood-Basalt Province, v. 239, p. 209-222.

Carmignani, L., Conti, P., Disperati, L., Fantozzi, P.L., Giglia, G., and Meccheri, M., 2000, Carta geologica del Parco delle Alpi Apuane, Parco delle Alpi Apuane (Ed.): Florence, S.E.L.C.A.

Carmignani, L., Decandia, F.A., Fantozzi, P.L., Lazzarotto, A., Liotta, D., and Meccheri, M., 1994, Tertiary extensional tectonics in Tuscany (Northern Apennines, Italy): Tectonophysics, v. 238, p. 295-&.

Carmignani, L., Giglia, G., and Kligfield, R., 1978, Structural evolution of the Apuane Alps: an example of continental margin deformation in the Northern Apennines, Italy: The Journal of Geology, p. 487-504.

Carmignani, L., and Kligfield, R., 1990, Crustal extension in the Northern Apennines - the transition from compression to extension in the Alpi Apuane core complex: Tectonics, v. 9, p. 1275-1303.

Carosi, R., Cerbai, N., and Montomoli, C., 1996, The F2 folds in the Verrucano as records of extensional tectonics in the Northern Apennines (Italy): Comptes rendus de l'Académie des sciences. Série 2. Sciences de la terre et des planètes, v. 322, p. 773-780.

Carosi, R., Montomoli, C., and Pertusati, P.C., 2002, Late orogenic structures and orogen-parallel compression in the Northern Apennines: Bollettino della Società geologica italiana, v. 121, p. 167-180.

Carosi, R., Montomoli, C., and Pertusati, P.C., 2004, Late tectonic evolution of the Northern Apennines: the role of contractional tectonics in the exhumation of the Tuscan Units: Geodinamica Acta, v. 17, p. 253-273.

Carter, K.E., Dworkin, S.I., Carmignani, L., Meccheri, M., and Fantozzi, P., 1994, Dating Thrust Events Using $^{87}Sr/^{86}Sr$: An Example from the Northern Apennines, Italy: The Journal of Geology, v. 102, p. 297-305.

Cashman, S.M., and Whetten, J.T., 1976, Low-temperature serpentinization of peridotite fanglomerate on the west margin of the Chiwaukum graben, Washington: Geological Society of America Bulletin, v. 87, p. 1773-1776.

Catchings, R., and Mooney, W., 1988, Crustal structure of the Columbia Plateau: Evidence for continental rifting: Journal of Geophysical Research, v. 93, p. 459-474.

Catchings, R., and Saltus, R., 1994, Upper-crustal structure beneath the Columbia River Basalt Group, Washington: Gravity interpretation controlled by borehole and seismic studies: Discussion and reply: Geological Society of America Bulletin, v. 106, p. 1096-1101.

Cello, G., and Mazzoli, S., 1996, Extensional processes driven by large-scale duplexing in collisional regimes: Journal of Structural Geology, v. 18, p. 1275-1279.

Cheney, E.S., and Hayman, N., 2009, The Chiwaukum Structural Low: Cenozoic shortening of the central Cascade Range, Washington State, USA: Geological Society of America Bulletin, v. 121, p. 1135-1153.

Coli, M., 1989, Time and mode of uplift of the Apuane Alps metamorphic complex: Atti Ticinesi Scienze della Terra, v. 32, p. 47-56.

Costa, E., Di Giulio, A., Pleuger, J., and Villa, G., 1992, Caratteri biostratigrafici e petrografici del Macino lungo la trasversale Cinque Terre-val Gordana-M. Sillaba (Appennino Setterntrionale): Implicazioni sull'evoluzione tettono-sedimentaria: GStudi Geol. Camerti, v. CROP 01-1A, p. 229-248.

Costagliola, P., Benvenuti, M., Maineri, C., Lattanzi, P., and Ruggieri, G., 1999, Fluid circulation in the Apuane Alps core complex; evidence from extension veins in the Carrara Marble: Mineralogical Magazine, v. 63, p. 111-122.

Cowan, D.S., and Brandon, M.T., 1994, A symmetry-based method for kinematic analysis of large-slip brittle fault zones: American Journal of Science, v. 294, p. 257-306.

Dallan Nardi, L., 1979, Microfossili miocenici nella matrice sedimentaria delle brecce situate alla base della "Falda Toscana" nelle Apuane meridionali: Boll. Soc. Geol. It, v. 98, p. 119-128.

Dallan Nardi, L., and Nardi, R., 1973, Ipotesi sulla genesi e sul significato delle brecce stratigrafiche associate ai "Calcari cavernosi" sulle Alpi Apuane e sul Monte Pisano in rapporto alla messa in posto della Falda Toscana: Boll. Soc. Geol. It, v. 92, p. 435-452.

Dallan-Nardi, L., 1977, Segnalazione di lepidocycline nella parte basale dello ''pseudomacigno''delle Alpi Apuane: Boll. Soc. Geol. Ital, v. 95, p. 459-477.

Decandia, A., Federici, P., and Giglia, G., 1968, Contributo alla conoscenza della serie Toscana: la zona di Castelpoggio e Tenerano (Carrara Alpi Apuane): Atti Soc. Tosc. Sc. Nat., Mem., sez. A, v. 75.

de Capoa, P., Radoicic, R., and D'Argenio, B., 1995, Late Miocene deformation of the External Dinarides (Montenegro and Dalmatia). New biostratigraphic evidence: Memorie di Scienze Geologiche, v. 47, p. 157-172.

Dewey, J., 1988, Extensional collapse of orogens: Tectonics, v. 7, p. 1123-1139.

Di Pisa, A., Franceschelli, M., Leoni, L., and Meccheri, M., 1985, Regional variation of the metamorphic temperature across the Tuscanid I Unit and its implication on the alpine metamorphism (Apuane Alps, N. Tuscany). Neues Jahrbuch Fur Mineralogie Abhandlungen, v. 151, p. 197-211.

Elter, P., Giannini, E., Tongiorgi, M., and Trevisan, L., 1960, Le varie unità tettoniche della Toscana e della Liguria orientale: Rend. Accad. Naz. Lincei Cl. Sc. Fis. Mat. Nat., serie, v. 8, p. 497-502.

Erslev, E.A., 1986, Basement balancing of Rocky Mountain foreland uplifts: Geology, v. 14, p. 259-262.

Evans, J.E., 1994, Depositional history of the Eocene Chumstick Formation: Implications of tectonic partitioning for the history of the Leavenworth and Entiat-Eagle Creek fault systems, Washington: Tectonics, v. 13, p. 1425-1444.

Faccenna, C., Davy, P., Brun, J.P., Funiciello, R., Giardini, D., Mattei, M., and Nalpas, T., 1996, The dynamics of back-arc extension: an experimental approach to the opening of the Tyrrhenian Sea: Geophysical Journal International, v. 126, p. 781-795.

Fazzuoli, M., Pandeli, E., and Sani, F., 1994, Considerations on the sedimentary and structural evolution of the Tuscan Domain since early Liassic to Tortonian: Mem. Soc. Geol. It, v. 48, p. 31-50.

Federici, P.R., and Raggi, G., 1974, Brecce Sedimentarie e Rapporti Tra Le Unita' Tettoniche Toscane Nel Gruppo Delle Alpi Apuane: Boll. Soc. Geol. It., v. 93, p. 709-722.

Fellin, M.G., Reiners, P.W., Brandon, M.T., Wuthrich, E., Balestrieri, M.L., and Molli, G., 2007, Thermochronologic evidence for the exhumational history of the Alpi Apuane metamorphic core complex, northern Apennines, Italy: Tectonics, v. 26, p. 22.

Feroni, A., Nutti, S., Pertusati, P.C., and Plesi, G., 1976, Sulla Probabile Origine Carsica Delle Brecce Sedimentarie Associate al Calcare Cavernoso Dell'Appennino Settentrionale: Boll. Soc. Geol. It., v. 95, p. 1161-1174.

Ferrill, D.A., 1991, Calcite twin widths and intensities as metamorphic indicators in natural low-temperature deformation of limestone: Journal of Structural Geology, v. 13, p. 667-675.

Ferrill, D.A., Morris, A.P., Evans, M.A., Burkhard, M., Groshong Jr, R.H., and Onasch, C.M., 2004, Calcite twin morphology: a low-temperature deformation geothermometer: Journal of Structural Geology, v. 26, p. 1521-1529.

Foster, D.A., and John, B.E., 1999, Quantifying tectonic exhumation in an extensional orogen with thermochronology: examples from the southern Basin and Range Province: Geological Society London Special Publications, v. 154, p. 343.

Franceschelli, M., Leoni, L., Memmi, I., and Puxeddu, M., 1986, Regional distribution of Al-silicates and metamorphic zonation in the low-grade Verrucano metasediments from the Northern Apennines, Italy: Journal of metamorphic Geology, v. 4, p. 309-321.

Galdenzi, S., and Maruoka, T., 2003, Gypsum deposits in the Frasassi Caves, central Italy: Journal of Cave and Karst Studies, v. 65, p. 111-125.

Gandin, A., Giamello, M., Guasparri, G., Mugnaini, S., and Sabatini, G., 2000, The Calcare Cavernoso of the Montagnola Senese (Siena, Italy): mineralogical–petrographic and petrogenetic features: Mineralogica et Petrographica Acta, v. 43, p. 271-289.

Giannini, E., Nardi, R., and Tongiorgi, M., 1962, Osservazioni sul problema della falda toscana: Boll. Soc. Geol. It, v. 81, p. 17-98.

Goff, F., 1981, Preliminary geology of eastern Umtanum Ridge, south-central Washington, Rockwell International, Rockwell Hanford Operations, Energy Systems Group.

Groshong Jr, R.H., Teufel, L., and Gasteiger, C., 1984, Precision and accuracy of the calcite strain-gage technique: Geological Society of America Bulletin, v. 95, p. 357-363.

Hagood, M.C., 1986, Structure and evolution of the Horse Heaven Hills in south-central Washington, Basalt Waste Isolation Program, Rockwell International, Rockwell Hanford Operations.

Hames, W., and Bowring, S., 1994, An empirical evaluation of the argon diffusion geometry in muscovite: Earth and Planetary Science Letters, v. 124, p. 161-169.

Harrison, T.M., and McDougall, I., 1981, Excess40Ar in metamorphic rocks from Broken Hill, New South Wales: implications for40Ar/39Ar age spectra and the thermal history of the region: Earth and Planetary Science Letters, v. 55, p. 123-149.

Hodgkins, M.A., and Stewart, K.G., 1994, The use of fluid inclusions to constrain fault zone pressure, temperature and kinematic history: an example from the Alpi Apuane, Italy: Journal of Structural Geology, v. 16, p. 85-96.

Ilic, A., and Neubauer, F., 2005, Tertiary to recent oblique convergence and wrenching of the Central Dinarides: Constraints from a palaeostress study: Tectonophysics, v. 410, p. 465-484.

Jarchow, C.M., Catchings, R.D., and Lutter, W.J., 1994, Large-explosive source, wide-recording aperture, seismic profiling on the Columbia Plateau, Washington: Geophysics, v. 59, p. 259-271.

Johnson, S.Y., 1985, Eocene strike-slip faulting and nonmarine basin formation in Washington: Strike-slip deformation, basin formation, and sedimentation, v. 37, p. 283-302.

Jolivet, L., Faccenna, C., Goffe, B., Mattei, M., Rossetti, F., Brunet, C., Storti, F., Funiciello, R., Cadet, J.P., d'Agostino, N., and Parra, T., 1998, Midcrustal shear zones in post-orogenic extension: Example from the northern Tyrrhenian Sea: Journal of Geophysical Research-Solid Earth, v. 103, p. 12123-12160.

Jolivet, L., and Brun, J.P., 2010, Cenozoic geodynamic evolution of the Aegean: International Journal of Earth Sciences, v. 99, p. 109-138.

Jovanović, R., M. Mojićević, S. Tokić, Lj. Rokić (1977), Basic geologic map sheet of Yugoslavia 1:100,000, sheet Sarajevo K 34-1, Fed. Geol. Inst., Beograd.

Kligfield, R., Hunziker, J., Dallmeyer, R., and Schamel, S., 1986, Dating of deformation phases using K-Ar and $^{40}Ar/^{39}Ar$ techniques: results from the Northern Apennines: Journal of Structural Geology, v. 8, p. 781-798.

Lugli, S., 2001, Timing of post-depositional events in the Burano Formation of the Secchia valley (Upper Triassic, Northern Apennines), clues from gypsum-anhydrite transitions and carbonate metasomatism: Sedimentary Geology, v. 140, p. 107-122.

Lugli, S., Morteani, G., and Blamart, D., 2002, Petrographic, REE, fluid inclusion and stable isotope study of magnesite from the Upper Triassic Burano Evaporites (Secchia Valley,

northern Apennines): contributions from sedimentary, hydrothermal and metasomatic sources: Mineralium Deposita, v. 37, p. 480-494.

Malavieille, J., Guihot, P., Costa, S., Lardeaux, J., and Gardien, V., 1990, Collapse of the thickened Variscan crust in the French Massif Central: Mont Pilat extensional shear zone and St. Etienne Late Carboniferous basin: Tectonophysics, v. 177, p. 139-149.

Malinverno, A., and Ryan, W.B.F., 1986, Extension in the Tyrrhenian sea and shortening in the Apennines as result of arc migration driven by sinking of the lithosphere: Tectonics, v. 5, p. 227-245.

Mandic, O., Paveli, D., Harzhauser, M., Zupani, J., Reischenbacher, D., Sachsenhofer, R.F., Tadej, N., and Vranjkovi, A., 2009, Depositional history of the Miocene Lake Sinj (Dinaride Lake System, Croatia): a long-lived hard-water lake in a pull-apart tectonic setting: Journal of Paleolimnology, v. 41, p. 431-452.

Martini, I., 2011, Cave clastic sediments and implications for speleogenesis: New insights from the Mugnano Cave (Montagnola Senese, Northern Apennines, Italy): Geomorphology.

Mauffret, A., Contrucci, I., and Brunet, C., 1999, Structural evolution of the Northern Tyrrhenian Sea from new seismic data: Marine and Petroleum Geology, v. 16, p. 381-407.

Mazzotti, S., Dragert, H., Hyndman, R.D., Miller, M.M., and Henton, J.A., 2002, GPS deformation in a region of high crustal seismicity: N. Cascadia forearc: Earth and Planetary Science Letters, v. 198, p. 41-48.

McCaffrey, R., Long, M.D., Goldfinger, C., Zwick, P.C., Nabelek, J.L., Johnson, C.K., and Smith, C., 2000, Rotation and plate locking at the southern Cascadia subduction zone: Geophys. Res. Lett, v. 27, p. 3117-3120.

McCaffrey, R., Qamar, A.I., King, R.W., Wells, R., Khazaradze, G., Williams, C.A., Stevens, C.W., Vollick, J.J., and Zwick, P.C., 2007, Fault locking, block rotation and crustal deformation in the Pacific Northwest: Geophysical Journal International, v. 169, p. 1315-1340.

Merla, G., 1951, Geologia dell'Appennino settentrionale: Bolletino Societa Geologic Italiana, v. 70, p. 95-382.

Mikes, T., Baldi-Beke, M., Kazmer, M., Dunkl, I., and von Eynatten, H., 2008, Calcareous nannofossil age constraints on Miocene flysch sedimentation in the Outer Dinarides (Slovenia, Croatia, Bosnia-Herzegovina and Montenegro): Geological Society London Special Publications, v. 298, p. 335.

Miller, R.B., and Bowring, S.A., 1990, Structure and chronology of the Oval Peak batholith and adjacent rocks: Implications for the Ross Lake fault zone, North Cascades, Washington: Geological Society of America Bulletin, v. 102, p. 1361-1377.

Molli, G., Conti, P., Giorgetti, G., Meccheri, M., and Oesterling, N., 2000, Microfabric study on the deformational and thermal history of the Alpi Apuane marbles (Carrara marbles), Italy: Journal of Structural Geology, v. 22, p. 1809-1825.

Molli, G., Giorgetti, G., and Meccheri, M., 2000, Structural and petrological constraints on the tectono-metamorphic evolution of the Massa Unit (Alpi Apuane, NW Tuscany, Italy): Geological Journal, v. 35, p. 251-264.

Molli, G., Giorgetti, G., and Meccheri, M., 2002, Tectono-metamorphic evolution of the Alpi Apuane Metamorphic Complex: new data and constraints for geodynamic models: Bollettino della Società geologica italiana, v. 121, p. 789-800.

Montanari, L., and Rossi, M., 1983, Evoluzione delle unità stratigrafico-strutturali terziarie del nord-appennino. 2. Macigno ss. e Pseudomacigno. Muovi dati cronostratigrafici e loro implicazioni.: Memorie Soceta Geologic Italiana, v. 25, p. 185-217.

Ottria, G., and Molli, G., 2000, Superimposed brittle structures in the late-orogenic extension of the Northern Apennine: results from the Carrara area (Alpi Apuane, NW Tuscany): Terra Nova, v. 12, p. 52-59.

Pamić, J., 1993, Eoalpine to Neoalpine magmatic and metamorphic processes in the northwestern Vardar Zone, the easternmost Periadriatic Zone and the southwestern Pannonian Basin: Tectonophysics, v. 226, p. 503-518.

Pamic, J., Balogh, K., Hrvatovic, H., Balen, D., Jurkovic, I., and Palinkas, L., 2004, K-Ar and Ar-Ar dating of the palaeozoic metamorphic complex from the Mid-Bosnian Schist Mts., central Dinarides, Bosnia and Hercegovina: Mineralogy and Petrology, v. 82, p. 65-79.

Pamic, J., Gusic, I., and Jelaska, V., 1998, Geodynamic evolution of the central Dinarides: Tectonophysics, v. 297, p. 251-268.

Pamic, J., and Jurkovic, I., 2002, Paleozoic tectonostratigraphic units of the northwest and central Dinarides and the adjoining South Tisia: International Journal of Earth Sciences, v. 91, p. 538-554.

Passchier, C.W., and Trouw, R.A.J., 2005, Microtectonics, Springer Verlag.

Patacca, E., Rau, A., and Tongiorgi, M., 1973, Il significato geologico della breccia sedimentaria poligenica al tetto della successione metamorfica dei Monti Pisani: Tosc. Sci. Nat. Mem., Serie A, v. 80, p. 126-161.

Paterson, S.R., Miller, R.B., Alsleben, H., Whitney, D.L., Valley, P.M., and Hurlow, H., 2004, Driving mechanisms for > 40 km of exhumation during contraction and extension in a continental arc, Cascades core, Washington: Tectonics, v. 23, p. TC3005.

Picha, F.J., 2002, Late orogenic strike-slip faulting and escape tectonics in frontal Dinafides-Hellenides, Croatia, Yugoslavia, Albania, and Greece: AAPG bulletin, v. 86, p. 1659-1671.

Piromallo, C., and Morelli, A., 2003, P wave tomography of the mantle under the Alpine-Mediterranean area: J. Geophys. Res, v. 108.

Platt, J.P., Behrmann, J.H., Cunningham, P.C., Dewey, J.F., Helman, M., Parish, M., Shepley, M.G., Wallis, S., and Weston, P.J., 1989, Kinematics of the Alpine arc and the motion history of Adria: Nature, v. 337, p. 158-161.

Radke, B.M., and Mathis, R.L., 1980, On the formation and occurrence of saddle dolomite: Journal of Sedimentary Research, v. 50, p. 1149-1168.

Reidel, S.P., 1984, The Saddle Mountains; the evolution of an anticline in the Yakima fold belt: American Journal of Science, v. 284, p. 942-978.

Reidel, S., 1988, Geologic map of the Saddle Mountains, south-central Washington, Washington, Division of Geology and Earth Resources.

Reidel, S., Fecht, K., Hagood, M., and Tolan, T., 1989, The geologic evolution of the central Columbia Plateau: Volcanism and Tectonism in the Columbia River Flood-Basalt Province, p. 247-264.

Reidel, S.P., and Fecht, K., 1994, Geologic map of the Priest Rapids 1:100,000 quadrangle, Washington Division of Geology and Earth Resources, Washington State Department of Natural Resources.

Reiners, P.W., 2005, Zircon (U-Th)/He thermochronometry: Reviews in mineralogy and geochemistry, v. 58, p. 151-179.

Reiners, P.W., and Brandon, M.T., 2006, Using thermochronology to understand orogenic erosion: Annual Review of Earth and Planetary Sciences, v. 34, p. 419-466.

Rey, P., Vanderhaeghe, O., and Teyssier, C., 2001, Gravitational collapse of the continental crust: definition, regimes and modes: Tectonophysics, v. 342, p. 435-449.

Rosenbaum, G., and Lister, G.S., 2004, Neogene and Quaternary rollback evolution of the Tyrrhenian Sea, the Apennines, and the Sicilian Maghrebides: Tectonics, v. 23.

Rowan, M.G., and Linares, R., 2000, Fold-evolution matrices and axial-surface analysis of fault-bend folds: application to the Medina anticline, Eastern Cordillera, Colombia: AAPG Bulletin, v. 84, p. 741-764.

Rowe, K.J., and Rutter, E.H., 1990, Palaeostress estimation using calcite twinning: experimental calibration and application to nature: Journal of Structural Geology, v. 12, p. 1-17.

Royden, L.H., 1993, Evolution of retreating subduction boundaries formed during continental collision: Tectonics, v. 12, p. 629-638.

Saftic, B., Velic, J., Sztano, O., Juhasz, G., and Ivkovic, Z., 2003, Tertiary Subsurface Facies, Source Rocks and Hydrocarbon Reservoirs in the SW Part of the Pannonian Basin (Northern Croatia and South-Western Hungary): Geologia Croatica, v. 56, p. 101-122.

Saltus, R., 1993, Upper-crustal structure beneath the Columbia River Basalt Group, Washington: Gravity interpretation controlled by borehole and seismic studies: Geological Society of America Bulletin, v. 105, p. 1247-1259.

Salvini, F., and Storti, F., 2001, The distribution of deformation in parallel fault-related folds with migrating axial surfaces: comparison between fault-propagation and fault-bend folding: Journal of Structural Geology, v. 23, p. 25-32.

Savage, H.M., and Cooke, M.L., 2003, Can flat-ramp-flat fault geometry be inferred from fold shape?: A comparison of kinematic and mechanical folds: Journal of Structural Geology, v. 25, p. 2023-2034.

Schmid, S.M., Bernoulli, D., Fügenschuh, B., Matenco, L., Schefer, S., Schuster, R., Tischler, M., and Ustaszewski, K., 2008, The Alpine-Carpathian-Dinaridic orogenic system: correlation and evolution of tectonic units: Swiss Journal of Geosciences, v. 101, p. 139-183.

Sani, F., 1985, Le brecce della Versilia tra successione toscana metamorfica e Falda Toscana nell'area di Casoli-Metato (Apuane meridionali): Rend. Soc. Geol. It, v. 8, p. 25-29.

Stein, S., and Sella, G.F., 2006, Pleistocene change from convergence to extension in the Apennines as a consequence of Adria microplate motion: The Adria Microplate: GPS Geodesy, Tectonics, and Hazards, p. 21–34.

Suppe, J., 1983, geometry and kinematics of fault-bend folding: American Journal of Science, v. 283, p. 684-721.

Tabor, R.W., Waitt, R.B., Jr., Frizzell, V.A., Jr., Swanson, D.A., Byerly, G.R., and Bentley, R.D., 1982, Geologic map of the Wenatchee 1:100,000 quadrangle, central Washington: U.S. Geological Survey Miscellaneous Investigations Series Map I-1311, 26 p., 1 pl., scale 1:100,000.

Tabor, R.W., Frizzell, V.A., Jr., Whetten, J.T., Waitt, R.B., Swanson, D.A., Byerly, G.R., Booth, D.B., Hetherington, M.J., and Zartman, R.E., 1987, Geologic map of the Chelan 30-minute by 60-minute quadrangle, Washington: U.S. Geological Survey Miscellaneous Investigations Series Map I-1661, 1 sheet, scale 1:100,000, with 29 p. text.

Tabor, R., Frizzell Jr, V., Vance, J., and Naeser, C., 1984, Ages and stratigraphy of lower and middle Tertiary sedimentary and volcanic rocks of the central Cascades, Washington: Application to the tectonic history of the Straight Creek fault: Geological Society of America Bulletin, v. 95, p. 26-44.

Tari Kovacic, V., and Mrinjek, E., 1994, The role of Palaeogene clastics in the tectonic interpretation of Northern Dalmatia(Southern Croatia): Geologia Croatica, v. 47, p. 127-138.

Tari, V., 2002, Evolution of the northern and western Dinarides: a tectonostratigraphic approach: Stephan Mueller Special Publication Series, v. 1, p. 223-236.

Taylor, S.B., Johnson, S.Y., Fraser, G.T., and Roberts, J.W., 1988, Sedimentation and tectonics of the lower and middle Eocene Swauk Formation in eastern Swauk Basin, central Cascades, central Washington: Canadian Journal of Earth Sciences, v. 25, p. 1020–1036

Tolan, T.L., and Beeson, M.H., 1984, Intracanyon flows of the Columbia River Basalt Group in the lower Columbia River Gorge and their relationship to the Troutdale Formation: Geological Society of America Bulletin, v. 95, p. 463-477.

Tomljenovic, B., and Csontos, L., 2001, Neogene-quaternary structures in the border zone between Alps, Dinarides and Pannonian Basin (Hrvatsko zagorje and Karlovac Basins, Croatia): International Journal of Earth Sciences, v. 90, p. 560-578.

Ustaszewski, K., Kounoy, S., Schmid, S.M., Schaltegger, U., Krepp, W., Frank, and Fugenschuh, 2010, Evolution of the Adria-Europe plate boundary in the Northern Dinarides: From contintent-continent collision to back-arc extension.: Tectonics, v. 29.

Ustaszewski, K., Schmid, S.M., Fuegenschuh, B., Tischler, M., Kissling, E., and Spakman, W., 2008, A map-view restoration of the Alpine-Carpathian-Dinaridic system for the Early Miocene: Swiss Journal of Geosciences, v. 101, p. S273-S294.

Vlahovic, I., Tisljar, J., Velic, I., and Maticec, D., 2005, Evolution of the Adriatic carbonate platform: Palaeogeography, main events and depositional dynamics: Palaeogeography Palaeoclimatology Palaeoecology, v. 220, p. 333-360.

von Blanckenburg, F., and Davies, J.H., 1995, Slab breakoff - a model for syncollisional magmatism and tectonics in the Alps: Tectonics, v. 14, p. 120-131.

von Blanckenburg, F., and Davies, J.H., 1996, Feasibility of double slab breakoff (Cretaceous and tertiary) during the Alpine convergence: Eclogae Geologicae Helvetiae, v. 89, p. 111-127.

von Blanckenburg, F., Kagami, H., Deutsch, A., Oberli, F., Meier, M., Wiedenbeck, M., Barth, S., and Fischer, H., 1998, The origin of Alpine plutons along the Periadriatic Lineament: Schweizerische Mineralogische Und Petrographische Mitteilungen, v. 78, p. 55-66.

Vujnovic, L. (1980), Basic geologic map sheet of Yugoslavia 1:100,000, sheet Bugojno L 33-143, Fed. Geol. Inst., Beograd.

Watters, T.R., 1989, Periodically spaced anticlines of the Columbia Plateau, in Reidel, S.P., and Hooper, P.R., eds., Volcanism and tectonism in the Columbia River flood-basale province, Volume Special Paper 239: Boulder, CO, Geological Society of America.

Wells, D.L., and Coppersmith, K.J., 1994, New empirical relationships among magnitude, rupture length, rupture width, rupture area, and surface displacement: Bulletin of the Seismological Society of America, v. 84, p. 974-1002.

West, M., Ashland, F., Busacca, A., Berger, G., and Shaffer, M., 1996, Late Quaternary deformation, Saddle Mountains anticline, south-central Washington: Geology, v. 24, p. 1123-1126.

Wilkerson, S. M., Medwedeff, D.A., and Marshak, S., 1991, Geometrical modeling of fault-related folds: a pseudo-three-dimensional approach: Journal of Structural Geology, v. 13, p. 801-812.

Wilkerson, S. M., Apotria, T., and Farid, T., 2002, Interpreting the geologic map expression of contractional fault-related fold terminations: lateral/oblique ramps versus displacement gradients: Journal of Structural Geology, v. 24, p. 593-607.

Wolf, R., Farley, K., and Kass, D., 1998, Modeling of the temperature sensitivity of the apatite (U-Th)/He thermochronometer: Chemical Geology, v. 148, p. 105-114.

Wortel, M.J.R., and Spakman, W., 2000, Geophysics - Subduction and slab detachment in the Mediterranean-Carpathian region: Science, v. 290, p. 1910-1917.

Vita

Gabriele Casale grew up in Madison, WI. In 2003 he earned a Bachelor of Arts degree in Geology at the University of Minnesota. In 2006 he earned a Master of Science degree in Geological Sciences from the University of Washington. From 2006-2007 he studied at the University of Zagreb as a visiting Fullbright Scholar. He completed a three-month internship at the Upstream Research Center at ExxonMobil in Houston, Texas. In 2011 he began teaching structural geology at Appalachian State University in Boone, North Carolina. He earned a Doctor of Philosophy in Geological Sciences from the University of Washington.